Pflugers Arch - Eur J Physiol (2009) 459:159–181
DOI 10.1007/s00424-009-0715-6

SIGNALING AND CELL PHYSIOLOGY

Acid-evoked Ca^{2+} signalling in rat sensory neurones: effects of anoxia and aglycaemia

Michael Henrich · Keith J. Buckler

Received: 12 December 2008 / Revised: 30 July 2009 / Accepted: 14 August 2009 / Published online: 6 October 2009
© The Author(s) 2009. This article is published with open access at Springerlink.com

Abstract Ischaemia excites sensory neurones (generating pain) and promotes calcitonin gene-related peptide release from nerve endings. Acidosis is thought to play a key role in mediating excitation via the activation of proton-sensitive cation channels. In this study, we investigated the effects of acidosis upon Ca^{2+} signalling in sensory neurones from rat dorsal root ganglia. Both hypercapnic (pH_o 6.8) and metabolic–hypercapnic (pH_o 6.2) acidosis caused a biphasic increase in cytosolic calcium concentration ($[Ca^{2+}]_i$). This comprised a brief Ca^{2+} transient (half-time approximately 30 s) caused by Ca^{2+} influx followed by a sustained rise in $[Ca^{2+}]_i$ due to Ca^{2+} release from caffeine and cyclopiazonic acid-sensitive internal stores. Acid-evoked Ca^{2+} influx was unaffected by voltage-gated Ca^{2+}-channel inhibition with nickel and acid sensing ion channel (ASIC) inhibition with amiloride but was blocked by inhibition of transient receptor potential vanilloid receptors (TRPV1) with (*E*)-3-(4-*t*-butylphenyl)-*N*-(2,3-dihydrobenzo[*b*][1,4] dioxin-6-yl)acrylamide (AMG 9810; 1 μM) and *N*-(4-tertiarybutylphenyl)-4-(3-cholorphyridin-2-yl) tetrahydropryazine-1(2H)-carbox-amide (BCTC; 1 μM). Combining acidosis with anoxia and aglycaemia increased the amplitude of both phases of Ca^{2+} elevation and prolonged the Ca^{2+} transient. The Ca^{2+} transient evoked by combined acidosis, aglycaemia and anoxia was also substantially blocked by AMG 9810 and BCTC and, to a lesser extent, by amiloride. In summary, the principle mechanisms mediating increase in $[Ca^{2+}]_i$ in response to acidosis are a brief Ca^{2+} influx through TRPV1 followed by sustained Ca^{2+} release from internal stores. These effects are potentiated by anoxia and aglycaemia, conditions also prevalent in ischaemia. The effects of anoxia and aglycaemia are suggested to be largely due to the inhibition of Ca^{2+}-clearance mechanisms and possible increase in the role of ASICs.

Keywords Acidosis · Calcium regulation · Calcium signalling · Hypoxia · Sensory neurones · TRP channels · Capsaicin · Ischaemia

Introduction

Tissue ischaemia leads to rapidly declining oxygen levels and diminished capacity for oxidative phosphorylation. The consequential switch to anaerobic metabolism, to maintain cellular ATP production, results in increased generation of metabolic acid. This, in combination with the lack of perfusion, culminates in a rapidly developing tissue acidosis. For example, during myocardial ischaemia, pH_o falls to ≈6.8 within the first 8 min and ≈6.2 after 20 min [20, 21, 59, 109]. Tissue acidoses together with elevation of extracellular K^+, ATP and bradykinin are all thought to play a role in the excitation of sensory neurones within ischaemic tissue and the generation of ischaemic pain [5, 22, 24, 70, 76, 80, 85].

Electronic supplementary material The online version of this article (doi:10.1007/s00424-009-0715-6) contains supplementary material, which is available to authorized users.

M. Henrich · K. J. Buckler (✉)
Department of Physiology, Anatomy and Genetics,
University of Oxford,
Sherrington Building, Parks Road,
Oxford OX1 3PT, UK
e-mail: keith.buckler@dpag.ox.ac.uk

Present Address:
M. Henrich
Department of Anaesthesia, Intensive Care Medicine,
Pain Therapy, Justus-Liebig-University Giessen,
Rudolf-Buchheim-Str. 7,
35392 Giessen, Germany

Acid is thought to excite sensory neurones by activating pH-sensitive cation channels [12, 68]. Two main types of proton-gated cation channel have been found in sensory neurones: acid-sensing ion channels (ASICs) and the transient receptor potential vanilloid 1 receptor (TRPV1). ASICs are predominantly sodium selective and can be blocked by amiloride [46–48, 99]. The ASIC family contains four distinct genes, of which ASICs 1 and 3 are both expressed in sensory neurones [46–48, 100]. ASICs and, in particular, ASIC3 have been implicated in cardiac sensory neurone activation by ischaemia [10, 78]. Although thought to be primarily gated by protons, activation of ASIC3 may be further enhanced by the presence of lactate [41, 59]. TRPV1 is expressed predominantly in small sensory neurones from the dorsal root ganglia (DRG) [29, 33, 58, 60, 104, 111] and is a polymodal sensor. TRPV1 may be activated by capsaicin, heat, protons and proalgesic substances. This ability of TRPV1 to integrate both physical and chemical stimuli suggests that it plays a major role in pain transduction [16, 44, 82]. Unlike most ASICs, TRPV1 is highly permeable to both Na^+ and Ca^{2+} (P_{Ca}/P_{Na} between 1 and 10) [8, 32, 96, 97].

In addition to acting as pain sensors, sensory neurones also release neuropeptides during ischaemia (e.g. calcitonin gene-related peptide (CGRP) or substance P) which may act locally to modulate tissue function and/or blood flow within the ischaemic zone [37, 50]. Whilst electrical excitation of sensory nerves by acidosis/ischaemia most probably results directly from membrane depolarisation (due to activation of the above proton-gated cation channels), secretory responses are likely to be mediated via a rise in intracellular Ca^{2+}. There are numerous factors that could contribute to changes in $[Ca^{2+}]_i$ during ischaemia including voltage-gated Ca^{2+} entry secondary to electrical excitation, direct Ca^{2+} influx through proton-gated channels, Ca^{2+} release from internal stores and modulation of Ca^{2+} uptake, buffering or extrusion. In the present study, we have therefore investigated the effects of acidosis on intracellular Ca^{2+} regulation in small, capsaicin-sensitive, sensory neurones (15–30 μm) from cervicothoracic DRG. These neurones were exposed to four different acid stimuli with pH_o values 6.8, 6.2 (with and without lactate), and 5.0 simulating the initial phase of an ischaemic event, more prolonged ischaemia and an extreme acidosis of the type typically used to study acid-sensitive cation channel function in vitro. Using a pharmacological approach, we have characterised the Ca^{2+}-entry pathways and stores that contribute to elevation of $[Ca^{2+}]_i$ during acidosis. In addition, since anoxia and aglycaemia can also have profound effects on Ca^{2+} metabolism [34], we combined these stimuli with acidosis to more closely simulate ischaemic conditions and to investigate their collective effect on $[Ca^{2+}]_i$.

Materials and methods

Neurone dissociation

Adult Wistar rats of either sex aged between 6 and 8 weeks (130–170 g) were sacrificed by an overdose of halothane (4%). Cervicothoracic DRG (C_4-Th_6) were removed under sterile conditions and were immediately transferred into cooled (on ice) Ca^{2+}- and Mg^{2+}-free phosphate-buffered saline (PBS), pH 7.4. After cleaning the ganglia from surrounding tissue, the ganglia were incubated in an enzymic dispersion media comprising 10 mg/ml collagenase type I (208 U/mg, Worthington, CLS-1, MON4393), 1 mg/ml trypsin (9.3 U/mg, Sigma, T-4665), in PBS and with 60 μM $CaCl_2$ and 33 μM $MgCl_2$. The ganglia were incubated at 37°C for 35 min. Following enzyme treatment, the ganglia were washed once in PBS (Ca^{2+}- and Mg^{2+}-free) and once in Dulbecco's modified Eagle's medium (DMEM; containing 10% fetal bovine serum, 1.2 mM l glutamine), before mechanical trituration in 1.5 ml of DMEM. The dissociated cells were then washed twice by centrifugation (at 1,000×*g* for 5 min) followed by resuspension in fresh DMEM. Following the final wash, the cell pellet was resuspended in 500 μl basal TNB-100 containing protein–lipid complex (Biochrom, Berlin, Germany), penicillin (100 IU/ml), streptomycin (100 μg/ml) and 10 μM/ml nerve growth factor (TNB). Following a second trituration, the neurones were seeded onto poly-L-lysine and laminin-coated coverslips (6 mm in diameter) and incubated in sterile culture dishes in a humidified chamber at 37°C and 5% CO_2/95% air for 2 h. After this incubation period, a further 3-ml TNB was added to each culture dish. The neurones were then kept in the incubator for at least 30 min before being used for experiments. These neurones were typically used within 2 days of isolation.

Fluorescence measurements

Measurements of Fura-2 fluorescence were performed using a microspectrofluorometer based on an epifluorescence microscope (Nikon Diaphot 200, Japan) fitted with photomultiplier tubes (PMT; Thorn, EMI, UK) to detect emitted fluorescence and a motor driven monochromator (Cairn Instruments, Kent) with xenon lamp to provide the excitation light source. Fura-2 was excited alternately at 340 and 380 nm (±8 nm) for 250 ms at each wavelength with the cycle repeated at 1 Hz. Emitted fluorescence from Fura-2 was passed through a bandpass filter centre wavelength 510 nm (±20 nm). Bandpass filtered fluorescence was detected using a PMT air cooled to −20°C (Thorn, EMI, UK). The output from the PMT was integrated over each illumination period and recorded on a microcomputer using a micro CED1401 and Spike 4 software (Cambridge Electronic Design). For Fura-2, the ratio of fluorescence at 340 nm relative to that at 380 nm (*R*) was also calculated and recorded using Spike 4 software.

Selection and superfusion of neurones

Neurones were placed in a recording chamber with a volume of approximately 100 μl mounted on the stage of the epifluorescence microscope (see below). This chamber was perfused with solutions at a flow rate of approximately 2 ml min. Solutions were delivered from reservoirs kept in a water bath to the recording chamber via medical grade stainless steel tubing articulated by short sections of Pharmed tubing (Norton performance plastics, UK). A mechanically driven two-way tap which allowed a rapid change between two different solutions was placed within a few inches of the recording chamber. A heating coil was placed around a short section of tubing between the tap and the chamber to ensure solutions remained at 37°C. This arrangement allows rapid solution exchange and tight control over the gas content and temperature of solutions.

Neurones were observed and fluorescence recorded through a X40 fluorescence grade objective (n.a. 1.30). Sensory neurones were initially selected by soma size (15–30 μm) and then tested for a response (a robust increase in $[Ca^{2+}]_i$) to capsaicin. This capsaicin test was usually conducted at the end of the experiment and proved positive in >80% of the neurones selected by the above size criteria. Only capsaicin-positive neurones are included in this study.

Loading of neurones with Fura-2-AM

To introduce Fura-2 into neurones, they were incubated in either a 4-(2-hydroxyethyl)-1-piperazineethanesulfonic acid (HEPES) buffered saline (for in vivo calibrations) or a bicarbonate buffered saline (for experiments) containing 5 μM Fura-2-AM (Molecular Probes, Leiden, The Netherlands) at room temperature for 25 min in a dark chamber. The HEPES buffered saline used comprised (in millimolars): HEPES 20, glucose 11, KCl 4.5, $MgCl_2$ 1, $CaCl_2$ 2.5, and NaCl 117, pH 7.4 at room temperature.

In vivo calibration of Fura-2

Fura-2-loaded neurones (see above) were incubated in a high-K^+ zero-Ca^{2+} HEPES buffered solution (consisting of 150 mM KCl, 5 mM NaCl, 1 mM ethylenediaminetetraacetic acid and 1 mM ethylene glycol tetraacetic acid (EGTA)) containing 10 μM ionomycin (Sigma, Dorset, UK) for 10–20 min. After this incubation, the neurones were placed in a flow through incubation chamber mounted on the microspectrofluorometer and perfused with the same high-K^+ zero-Ca^{2+} HEPES solution but containing 1 μM ionomycin and at 37°C. After a further 5-min incubation in this solution, Fura-2 fluorescence was recorded from five identified sensory neurones. The ratio of fluorescence obtained under these conditions was deemed equivalent to the calibration constant $R_{\min}$ [30]. The perfusate was then changed to a high-K^+ high-Ca^{2+} HEPES saline containing 150 mM KCl, 5 mM NaCl, 10 mM $CaCl_2$ and 1 μM ionomycin. The change in fluorescence ratio was followed in one of the five identified neurones until it reached a new stable value, and then the fluorescence ratio in it and the other four identified neurones were recorded and deemed to be equivalent to the calibration constant $R_{\max}$. The ratio of fluorescence at 380 nm in Ca^{2+}-free buffer divided by that obtained in high Ca^{2+} buffer (S_{f2}/S_{b2}) was also calculated for each neurone. The mean values obtained for $R_{\min}$, $R_{\max}$ and (S_{f2}/S_{b2}) were then used to calibrate measurements of the fluorescence ratio in subsequent experiments using the equation $[Ca^{2+}]=(R-R_{\min})/(R_{\max}-R)\times S_{f2}/S_{b2}\times \mathrm{Kd}$ [30].

Solutions

The standard bicarbonate buffered Tyrode solutions contained (in millimolars) NaCl 117, KCl 4.5, $CaCl_2$ 2.5, $MgCl_2$ 1, HCO_3^- 23 and glucose 11. Glucose-free Tyrode solution was prepared by replacing glucose with 11 mM sucrose. For Ca^{2+}-free solution, the $CaCl_2$ was omitted and 1 mM EGTA was added. For Tyrode solution with elevated KCl concentration (50 mM), the NaCl concentration was reduced to 71.5 mM; all other constituents remained the same. Equilibration of these solutions with 5% CO_2 and 95% air achieved normocapnic conditions with pH 7.4 at 37°C. Moderate hypercapnic acidosis (pH_o 6.8) was achieved by increasing the CO_2 content of the equilibrating gas from 5% to 20%. To achieve a combined respiratory and metabolic acidosis, Tyrode solution with reduced $NaHCO_3$ (10 mM, 130 mM NaCl) was equilibrated with 20% CO_2, which resulted in a pH_o 6.2. pH 5.0 solutions were attained by lowering $NaHCO_3$ to 2 mM (and increasing NaCl to 138 mM) whilst equilibrating with 20% CO_2. Solutions simulating a lactic acidosis contained (in millimolars) Na-lactate 15, NaCl 126, KCl 4.5, $CaCl_2$ 2.5, $MgCl_2$ 1 and glucose 11. The pH of this solution was adjusted to 6.2 at 37°C by equilibration with 20% CO_2 and addition of NaOH.

Anoxic solutions were generated by replacing the air in the gas used to equilibrate the above solutions with nitrogen (i.e. gas mixtures were $x\%$ $CO_2+100-x\%$ N_2) and with the further addition of 0.5 mM $Na_2S_2O_4$ [72] following 15–30 min prior equilibration with the appropriate oxygen-free gas mixture. The addition of $Na_2S_2O_4$ did not cause any detectable change in solution pH. All solutions were equilibrated with appropriate gas mixes at 37°C in a water bath for at least 30 min before use.

Drugs

(*E*)-3-(4-*t*-butylphenyl)-*N*-(2,3-dihydrobenzo[*b*][1,4] dioxin-6-yl)acrylamide (AMG 9810, 1 μM), *N*-(4-tertiary-butylphenyl)-4-(3-cholorphyridin-2-yl) tetrahydropryazine-1 (2H)-carbox-amide (BCTC, 1 μM), capsazepine (CPZ; 10 μM), cyclopiazonic acid (CPA; 10 μM), carbonyl cyanide-*p*-trifluoromethoxyphenylhydrazone (FCCP; 1 μM) and amiloride (100 μM) containing solutions were prepared from stock solutions in dimethyl sulfoxide. Capsaicin was added from stock solutions in ethanol. $NiCl_2$ (2.5 mM), $CdCl_2$ (100 μM), $MnCl_2$ (1 mM) and $GdCl_3$ (0.5–1 mM) containing solutions were prepared from 0.5 to 1 M stock solutions in H_2O.

Statistics

Values were expressed as mean ± standard error of mean (SEM). Statistical significance was tested using the paired Student's *t* test, or Wilcoxon signed-rank test for experiments with non-Gaussian distribution. Statistical testing of in vitro calibration data was performed using one-way analysis of variance and post hoc analyses were carried out using Bonferroni's multiple comparison, calculated by SPSS 12.0 software for windows. Level of significance was set at $p<0.05$.

Results

Acidosis evoked rise in $[Ca^{2+}]_i$ in sensory neurones

Tissue acidosis is believed to be a major activator of sensory neurones transmitting ischaemic pain. Here, we investigated changes in $[Ca^{2+}]_i$ in response to acidosis. Four different types of acidosis were tested: 20% CO_2 in normal, 23 mM, HCO_3^- (pH_o 6.8) simulating a simple hypercapnic acidosis; 20% CO_2 in 10 mM HCO_3^- and 20% CO_2 in 15 mM Na-lactate (both pH_o 6.2) simulating a mixed hypercapnic and metabolic acidosis (with and without lactate ions present); and 20% CO_2 in 2 mM HCO_3^- (pH_o 5.0) simulating a very severe hypercapnic/metabolic acidosis.

In the majority of sensory neurones (65%) exposure to acidosis (either pH_o6.8, 6.2 or 5.0) evoked a rise in $[Ca^{2+}]_i$. This rise in $[Ca^{2+}]_i$ typically had a biphasic kinetic with an initial Ca^{2+} transient leading into a sustained elevation of $[Ca^{2+}]_i$ which remained throughout the exposure to acid (Fig. 1a). In a few neurones, however, only an initial Ca^{2+} transient was obvious with $[Ca^{2+}]_i$ returning back to baseline whilst still under acidic conditions (e.g. Fig. 1c). Another small subgroup of neurones lacked an obvious Ca^{2+} transient and instead responded with a rapid rise in $[Ca^{2+}]_i$ up to a plateau that was then sustained throughout exposure to acidosis (Fig. 1b).

The peak amplitudes of acid-induced Ca^{2+} transients were quantified as the maximal increase in $[Ca^{2+}]_i$ attained within the first minute of exposure to acidosis relative to baseline (e.g. Fig. 1c). The sustained elevation was defined as the averaged rise in $[Ca^{2+}]_i$ from the final 30 s of acidosis exposure relative to baseline (Fig. 1a). The $\Delta[Ca^{2+}]_i$ of the transients (Δ trans) were thus defined as the difference between the sustained elevation and the transient peak (e.g. Fig. 1a). A Ca^{2+} transient was only considered to have occurred where this $\Delta[Ca^{2+}]_i$ measurement was greater than the mean + 2 times the standard deviation of the sustained elevation in $[Ca^{2+}]_i$. The duration of the Ca^{2+} transient was characterised by measuring the time taken for the $[Ca^{2+}]_i$ to fall to half of the peak value ($t_{1/2}$).

In neurones responding with an initial Ca^{2+} transient, the mean Δtrans evoked by hypercapnic acidosis alone (pH_o 6.8) was 112±24.5 nM (n=10) and that evoked by a combined hypercapnic/metabolic acidosis (pH_o 6.2) was 871±352 nM (n=7). These acid-evoked Ca^{2+} transients were substantially attenuated in Ca_o^{2+}-free media to 7±0 nM (n=10, $^{**}p<0.01$) for a hypercapnic acidosis and 120±22 nM (n=7, $^{*}p<0.05$) for a combined hypercapnic/metabolic acidosis (see Fig. 1a, c, d). Thus, for both types of acid stimuli, the transient elevation in $[Ca^{2+}]_i$ in response to acidosis was strongly dependent upon the presence of extracellular Ca^{2+}. In contrast, the sustained rise in $[Ca^{2+}]_i$ was unaffected by Ca^{2+}-free solutions (see below). Acid-evoked Ca^{2+} transients were often relatively brief with $t_{1/2}$=27.8±1.1 s at pH_o 6.8 (n=27) and 28.1±1.3 s at pH_o 6.2 (n=27).

Acidosis due to tissue ischaemia is often accompanied by an increase in lactate from anaerobic respiration. Lactate has been reported to augment acid-evoked inward currents in sensory neurones [41]. We therefore compared a simple mixed acidosis (20% CO_2, pH 6.2) with an equivalent acidosis in the presence of 15 mM lactate (also 20% CO_2, pH 6.2). Eighty percent of neurones showed similar Ca^{2+} transients to both stimuli, and in these neurones, there was no significant difference between the amplitudes of these Ca^{2+} transients (Na-lactate 106±11%, n=26, p=0.442, data normalised to pH_o 6.2 with 20% CO_2; Fig. 1f). A few neurones responded only to one or other of the two stimuli.

Correlation between capsaicin- and acidosis-evoked Ca^{2+} transients

In this study, we have focussed upon sensory neurones selected by morphology and sensitivity to capsaicin. The capsaicin receptor (TRPV1) is also acid sensitive and

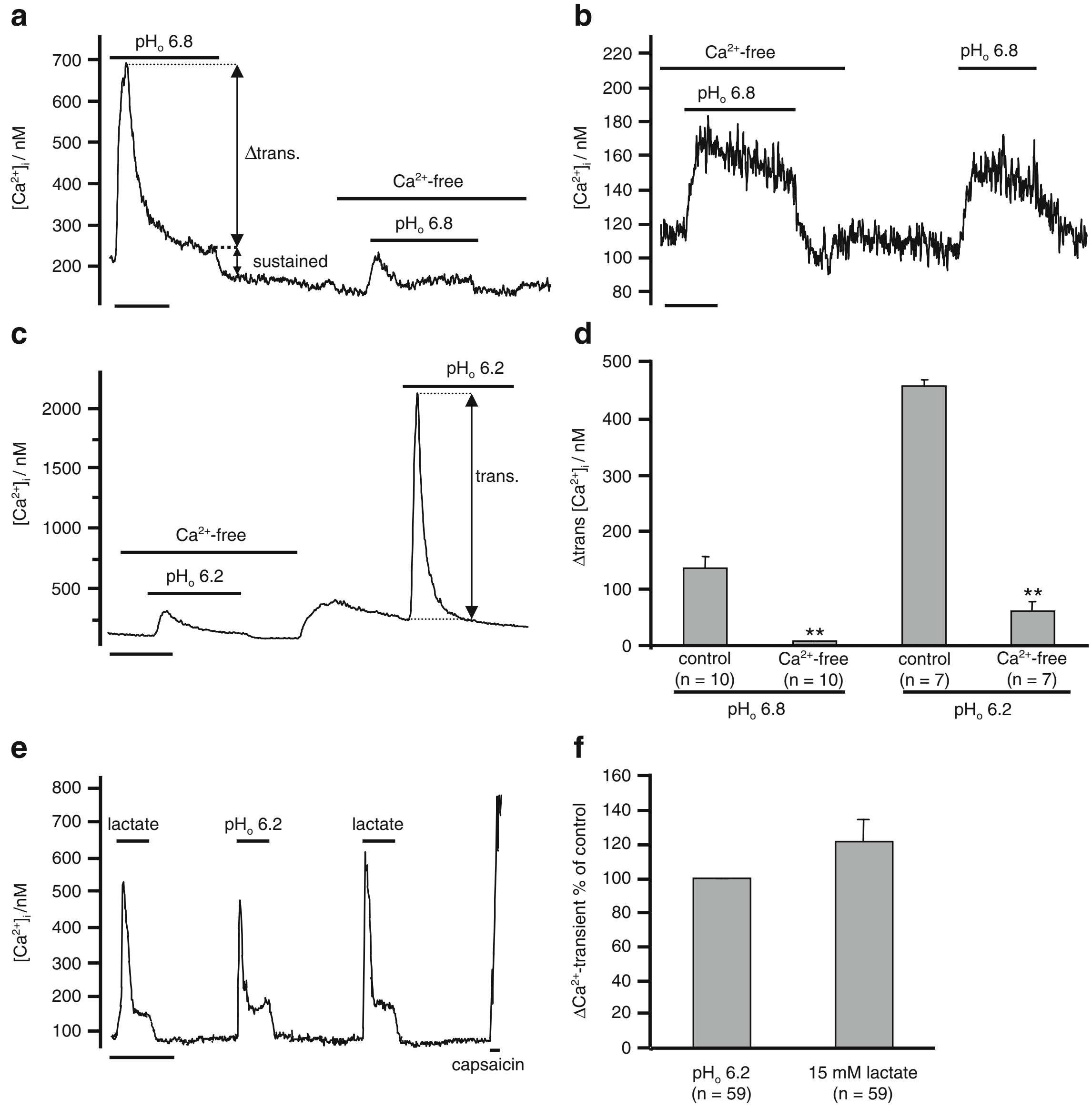

Fig. 1 Extracellular acidosis evokes rise in $[Ca^{2+}]_i$ in sensory neurones. **a**–**c** Effects of a hypercapnic (20% CO_2, pH_o 6.8) and a mixed acidosis (20% CO_2, pH_o 6.2) on $[Ca^{2+}]_i$ in capsaicin-sensitive neurones in the presence and absence of extracellular Ca^{2+}. In the presence of extracellular Ca^{2+}, acidosis evoked an initial transient followed by a sustained rise in $[Ca^{2+}]_i$ in the majority of neurones (e.g. **a** and **c**). The amplitude of this Ca^{2+}-transient amplitude was defined as the maximal increase in $[Ca^{2+}]_i$ within the first minute of exposure (see **c**). The amplitude of the sustained rise was defined as the mean increase in $[Ca^{2+}]_i$ during the final 30 s of the exposure period (see **a**). The $\Delta[Ca^{2+}]_i$ of the transients were thus defined as the difference between the sustained rise and the transient peak (Δtrans., see **a**). **d** Comparison of the amplitude of initial Ca^{2+} transients evoked by acidosis pH_o 6.8 or 6.2 in the presence and absence of extracellular Ca^{2+} (**p<0.01). **e**, **f** Comparison of Ca^{2+} responses evoked by mixed acidosis (20% CO_2, pH_o6.2) in the presence and absence of lactate (15 mM). **f** Comparison of the amplitude of the Ca^{2+} transient in response to lactic acidosis normalised to the response to acidosis in the absence of lactate. Time scale bars in **a**–**c** and **e** 200 s. Exposure periods are indicated by *horizontal bars*. *Bar charts* present means + SEM; numbers of experiments are given in *parenthesis*

would be expected to contribute to acid-evoked Ca^{2+} influx described above. We therefore sought to compare the amplitude of $[Ca^{2+}]_i$ responses to capsaicin (100 nM) with those evoked by acidosis. A significant positive correlation was observed between the amplitude of the Ca^{2+} transient evoked by capsaicin (100 nM) and that evoked by pH_o 6.8 (r=0.49, p<0.05, n=22) and pH_o 5.0 (r=0.69, p<0.05, n=11; Fig. 2a, c), but not by pH_o 6.2 (r=0.4, p=0.081, n=20; Fig. 2b). It is, however, evident that this correlation was not particularly strong. We also noted a striking paradox in that a significant number of neurones (approximately 15–20%) responding to capsaicin did not respond to acidosis with a transient Ca^{2+} influx. This failure to respond to acidosis could not be attributed to low levels of

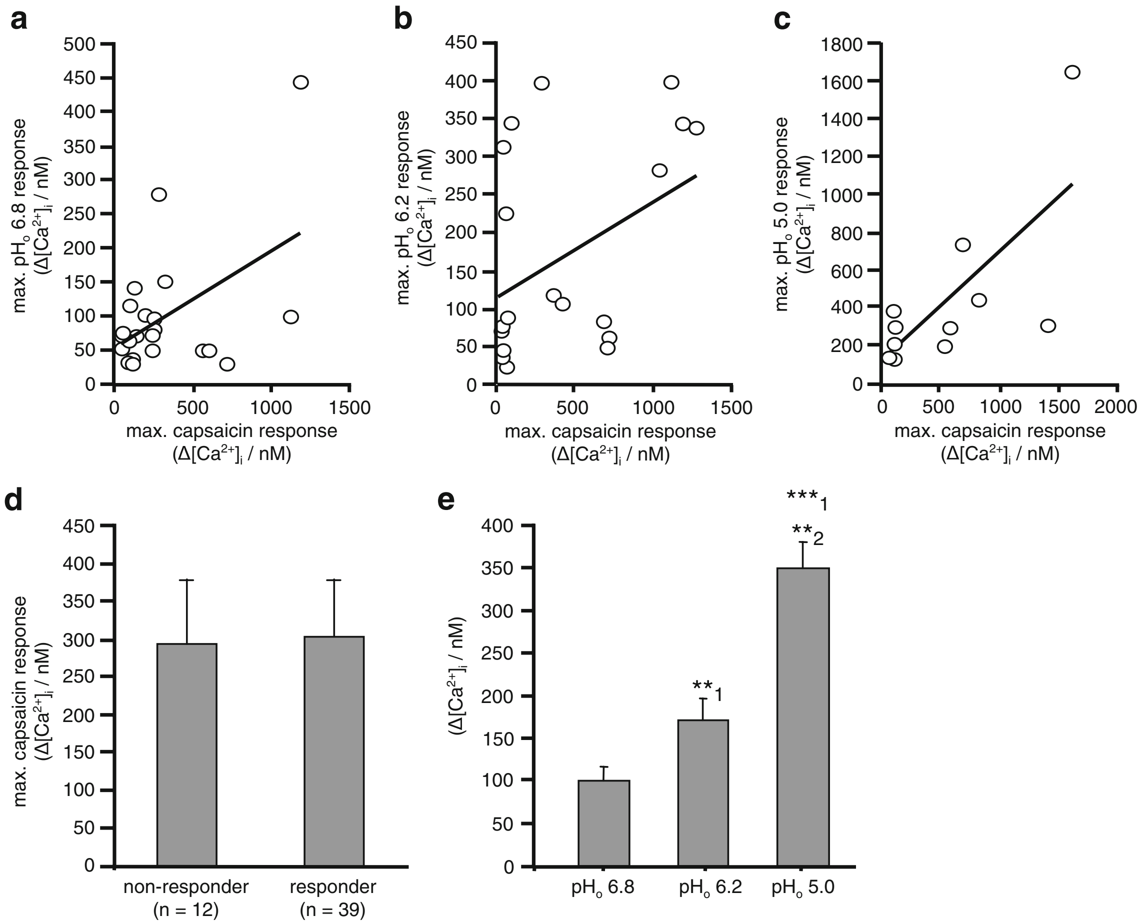

Fig. 2 Correlation between response to capsaicin and acidosis. **a**–**c** Correlation between maximum amplitudes of Ca^{2+} transients evoked by acidosis vs. capsaicin (100 nM). There was a weak positive correlation between the Ca^{2+} response to capsaicin and that to pH$_o$ 6.8 and 5.0 (r=0.49, p<0.05, n=22 for pH$_o$ 6.8; r=0.69, p<0.05, n=11 for pH$_o$5.0) but not pH$_o$ 6.2 (r=0.4, p=0.081, n=20). **d** The maximum amplitudes of $[Ca^{2+}]_i$ response to capsaicin (100 nM) in neurones responding (responder) or not responding (nonresponder) to external acidosis with a biphasic rise in $[Ca^{2+}]_i$. There was no difference in the $[Ca^{2+}]_i$ response to capsaicin in these two subgroups (p=0.886). **e** The amplitudes of Ca^{2+} transients evoked by extracellular acidosis significantly increase with falling pH$_o$ values (*1* compared to pH$_o$ 6.8; *2* compared to pH$_o$ 6.2; **p<0.01; ***p<0.001)

functional expression of the capsaicin receptor since we found no significant difference between the amplitude of the capsaicin-evoked Ca^{2+} transients in acid responders (308±78 nM, n=39) vs. acid nonresponders (295±86 nM, n=12, p=0.886; Fig. 2d). The importance of TRPV1 and other Ca^{2+} influx pathways in mediating acid-evoked Ca^{2+} influx was therefore investigated further.

Influence of divalent and trivalent cations on Ca^{2+}-entry pathways

The former experiments indicated that external acidosis has a dual action on $[Ca^{2+}]_i$. An initial Ca^{2+} transient was evoked by activation of a Ca^{2+}-entry pathway, whereas the sustained elevation of $[Ca^{2+}]_i$ was triggered independently from external Ca^{2+}.

In order to determine the Ca^{2+}-entry pathways involved in mediating the transient response to acidosis, we needed to find ways of selectively inhibiting the different types of Ca^{2+}-permeable channels that may be involved. Divalent and trivalent cations are often useful in this respect. Cd^{2+} is widely used to block voltage-gated Ca^{2+} channels especially in electrophysiological experiments. In these sensory neurones, Cd^{2+} (100 µM) similarly inhibited voltage-gated Ca^{2+} entry elicited by 50 mM KCl (by 89%±7%, n=5; Fig. 3a). The application of capsaicin in the presence of Cd^{2+} (100 µM), however, led to a rise in fluorescence ratio that exceeded that observed in the absence of Cd^{2+} and either did not recover or recovered only partially within the observation period (Fig. 3b). Removal of external Ca^{2+} failed to inhibit the effect of capsaicin in the presence of Cd^{2+} although it was inhibited by capsazepine (Fig. 3c).

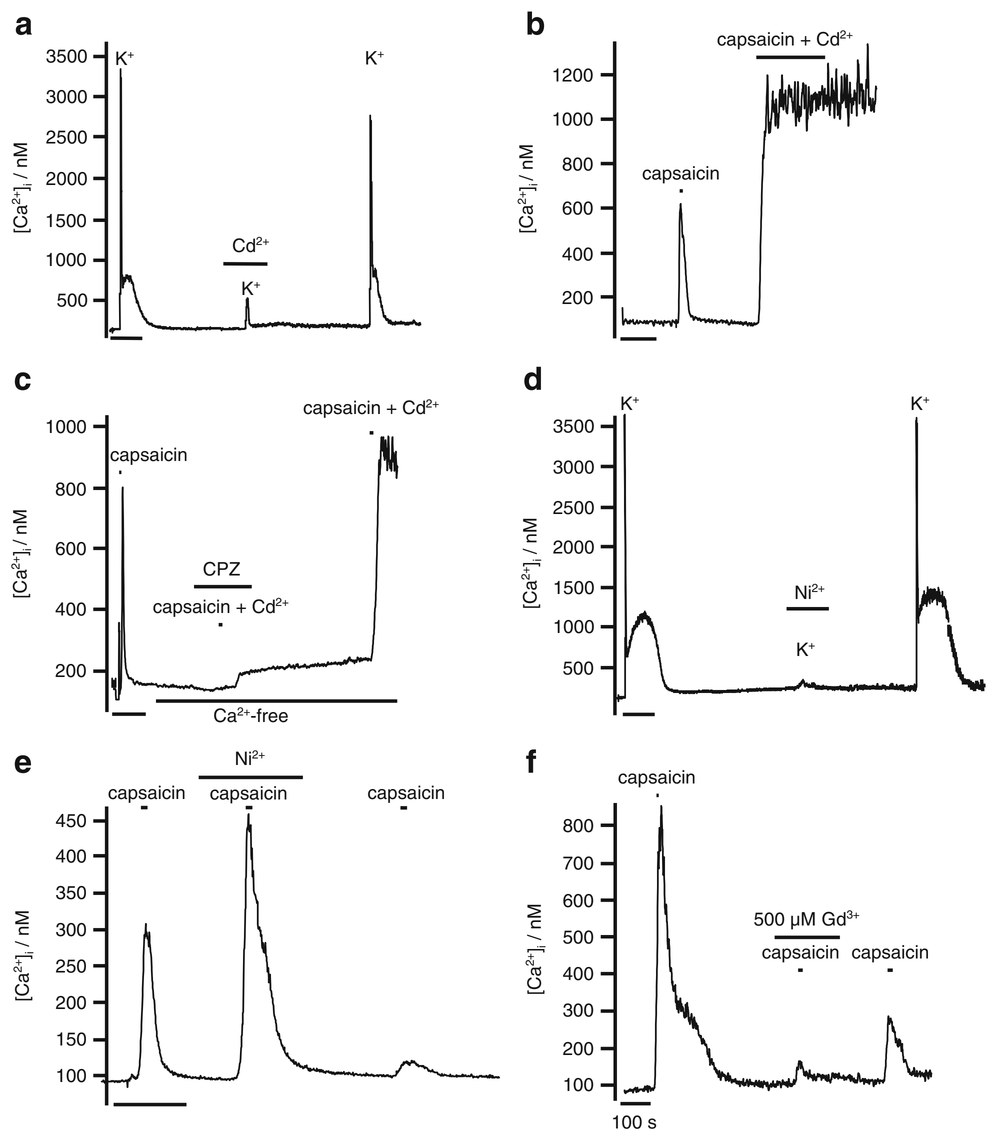

Fig. 3 Inhibition of Ca^{2+}-entry pathways by divalent and trivalent cations. **a** Voltage-gated Ca^{2+} entry triggered by KCl exposure (50 mM for 5 s) is almost fully inhibited by 100 μM Cd^{2+} (to 11% of control). **b** Application of Cd^{2+} (100 μM) in Ca^{2+}-containing solution amplified the $[Ca^{2+}]_i$ response to capsaicin (100 nM). Note also that the $[Ca^{2+}]_i$ response to capsaicin in the presence of Cd^{2+} often failed to fully recover. **c** In Ca^{2+}-free solution, capsazepine (10 μM) prevented a rise in Fura-2 fluorescence in response to capsaicin and Cd^{2+} application (note that following second exposure to capsaicin and Cd^{2+} in Ca^{2+}-free medium lacking capsazepine Fura-2 fluorescence increased dramatically and did not recover). **d** Inhibition of voltage-gated Ca^{2+} influx (50 mM KCl) by 2.5 mM Ni^{2+}. **e** Ni^{2+} (2.5 mM) enhanced Ca^{2+} transients evoked by capsaicin. **f** Gd^{3+} (0.5 mM) inhibited almost completely capsaicin evoked rise in $[Ca^{2+}]_i$. The response to capsaicin recovered partially during a final capsaicin application omitting Gd^{3+}. Exposure periods are indicated by *horizontal bars*. *Time scale bars*, 100 s

These data suggest that Cd^{2+} is able to permeate TRPV1 channels. Once inside the cell, Cd^{2+} will inevitably bind to Fura-2, as this has a much higher affinity for Cd^{2+} than for Ca^{2+}, which will cause similar changes in Fura-2 fluorescence to that observed with Ca^{2+} [36]. Thus, Cd^{2+} is inappropriate for use as a blocker of voltage-gated Ca^{2+} entry under conditions in which TRPV1 channels might be active (e.g. such as in responses to acidosis).

Ni^{2+} at relatively high (millimolars) concentrations can also be used to block voltage-gated Ca^{2+} entry [62]; 2.5 mM Ni^{2+} thus blocked high-K^+ (voltage-gated) Ca^{2+} influx (Fig. 3d) in these neurones but it did not inhibit the response to capsaicin; instead in the presence of Ni^{2+}, we measured a slightly enhanced rise in $[Ca^{2+}]_i$ (130±10%, n=5, compared to control; Fig. 3e). This enhanced response to capsaicin in the presence of Ni^{2+} recovered back to baseline after wash out of capsaicin (unlike that seen in the presence of Cd^{2+}). Mn^{2+} ions can also pass through many Ca^{2+} permeable channels and, upon gaining access to the cytosol, will quench Fura-2 fluorescence. Fura-2 fluorescence quenching by Mn^{2+} is therefore a useful technique with which to monitor the activation of various Ca^{2+}-entry pathways. As shown in Fig. 4a, 2.5 mM Ni^{2+} prevents high K^+-induced Fura-2 quenching by Mn^{2+} but does not prevent capsaicin induced Fura-2 quenching by Mn^{2+} (Fig. 4b). Ni^{2+} is therefore a good blocker of voltage-gated Ca^{2+} entry but has little effect upon Ca^{2+} or Mn^{2+} entry through TRPV1.

We next tested the effects of the trivalent cation Gd^{3+} upon the Ca^{2+} response evoked by capsaicin. Gd^{3+} (0.5 mM) substantially inhibited the $[Ca^{2+}]_i$ response to capsaicin (reduced to 6±4%, n=6, p<0.001 compared to control). This inhibition appeared to be only partially reversible (the third exposure to capsaicin following wash of gadolinium was 23±7%, n=6, p<0.01, compared to control; Fig. 3f). Gd^{3+} is therefore an effective inhibitor of

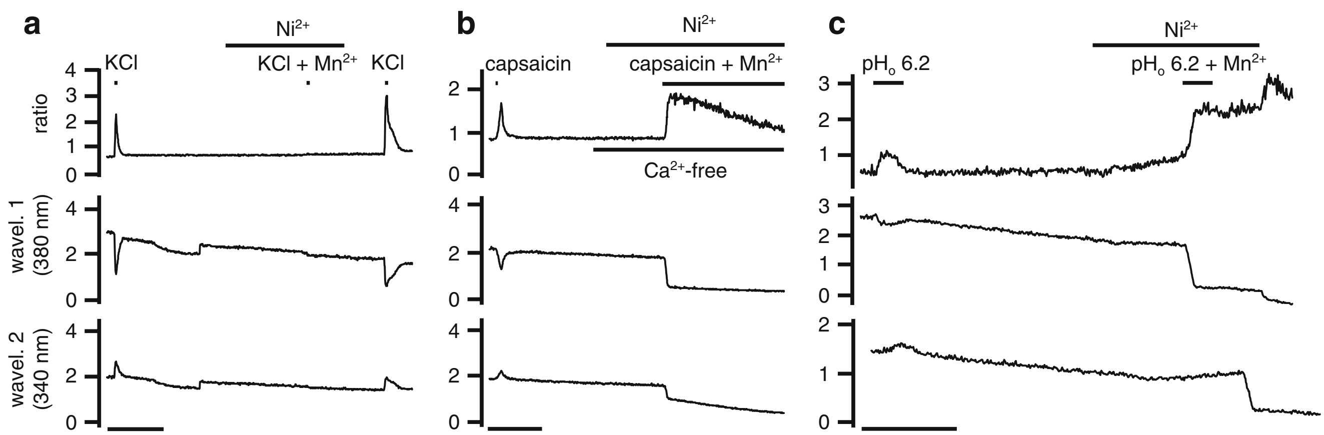

Fig. 4 Mn^{2+} quenching of Fura-2 fluorescence. This *figure* shows Fura-2 fluorescence at each individual excitation wavelength (340 and 380 nm) and the excitation ratio (340:380). In **a**, voltage-gated Ca^{2+} influx is triggered by brief depolarisation using KCl (50 mM for 5 s) causing a transient rise in Fura-2 fluorescence ratio. In the presence of Ni^{2+} (2.5 mM) to block voltage-gated Ca^{2+} channels, depolarisation by KCl in the presence of 1 mM Mn^{2+} (1 mM) does not cause quenching of Fura-2 fluorescence. Thus, Ni^{2+} blocks Mn^{2+} entry through voltage-gated Ca^{2+} channels. In **b**, application of capsaicin also evokes a transient rise of Fura-2 ratio. In Ca^{2+}-free solutions and in the presence of Ni^{2+} (2.5 mM) to block voltage-gated Ca^{2+} channels, the simultaneous application of capsaicin and Mn^{2+} (1 mM) resulted in a rapid quench of Fura-2 fluorescence at both wavelengths. Thus, activation of capsaicin receptors causes Mn^{2+} influx independently of voltage-gated Ca^{2+}-channel activity. **c** Exposure to acidosis (pH_o6.2) triggered a transient rise of Fura-2 ratio. In the presence of Ni^{2+} (2.5 mM) to block voltage-gated Ca^{2+} channels, the simultaneous exposure to acidosis (pH_o 6.2) and Mn^{2+} (1 mM) caused a immediate quench of Fura-2 fluorescence of both individual wavelengths. Exposure periods are indicated by *horizontal bars*. *Time scale bars*, 100 s

TRPV1-mediated Ca^{2+} entry although it lacks specificity, i.e. it also blocks voltage-gated Ca^{2+} channels [62]. Reversibility may also be slow[1].

In summary, Ni^{2+} blocks voltage-gated Ca^{2+} and Mn^{2+} entry, but not Ca^{2+} or Mn^{2+} influx through TRPV1. Gadolinium (0.5 mM) blocks both voltage-gated Ca^{2+} channels and TRPV1, and Cd^{2+} blocks voltage-gated Ca^{2+} entry but actually permeates TRPV1 sufficiently well to induce a major increase in Fura-2 fluorescence. These features can therefore be used to discriminate between a Ca^{2+}-influx pathway utilising voltage-gated channels and one using TRPV1.

Acidosis-activated Ca^{2+}-entry pathways in DRG neurones

In order to determine the route of Ca^{2+} entry in response to acidosis, we have studied the effects of a variety of pharmacological agents upon the amplitude of the Ca^{2+} transient generated at pH_o6.8, 6.2 and 5.0. In these experiments, control acid stimuli were applied before and after exposure to the pharmacological agent and the test acid stimulus; data were then normalised to the amplitude of the first control response (set as 100%).

Ni^{2+} failed to inhibit the Ca^{2+} transients evoked in response to pH_o 6.8, 6.2 or 5.0 (Fig. 5). Indeed, there was some evidence that at pH_o 6.2, Ni^{2+} enhanced the response to acidosis (276±42%, n=5, p<0.01) when compared to the first control. We also noted a tendency for the second, post-Ni^{2+}, control response (recovery) to be amplified relative to the first control (Fig. 5d) at pH_o6.8 (127±10%, n=6, p<0.05), 6.2 (230±87%, p<0.05, n=5) and 5.0 (248±62%, n=5, p<0.05). Acidosis (pH 6.2) also activated Mn^{2+} influx and Fura-2 fluorescence quenching in the presence of 2.5 mM Ni^{2+} (Fig. 4c).

Gadolinium (Gd^{3+}; 0.5 mM) completely blocked Ca^{2+} transients evoked by pH_o 6.8 in all neurones investigated (n=5) and almost completely blocked the response to pH_o 6.2 (only one neurone in five showed any response; Fig. 6). Gadolinium also suppressed the second control (recovery) response to pH_o 6.8 but not that to pH_o 6.2. Application of capsaicin (100 nM) at the end of each experiment and after a rest period of several minutes evoked robust Ca^{2+} transients confirming that any effects of Gd^{3+} upon TRPV1 channels were ultimately reversible (Fig. 6).

Application of acid stimuli in the presence of Cd^{2+} caused a massive rise in Fura-2 fluorescence that almost reached saturation (i.e. the maximal value for the fluorescence ratio encountered during Fura-2 calibration). Following removal of acidosis, the fluorescence ratio did not fully recover during the observation period (Fig. 6c). This observation is

[1] Note that whilst under control conditions we were usually able to obtain consistent Ca^{2+} responses to repeated applications of capsaicin (i.e. without obvious receptor desensitisation), we cannot exclude the possibility that lack of full recovery of the capsaicin response following application of Gd^{3+} could be due to enhanced desensitisation rather than persistent channel block per se. We also on occasion noted failure of the capsaicin response postapplication of Ni^{2+} (e.g. Fig. 3d).

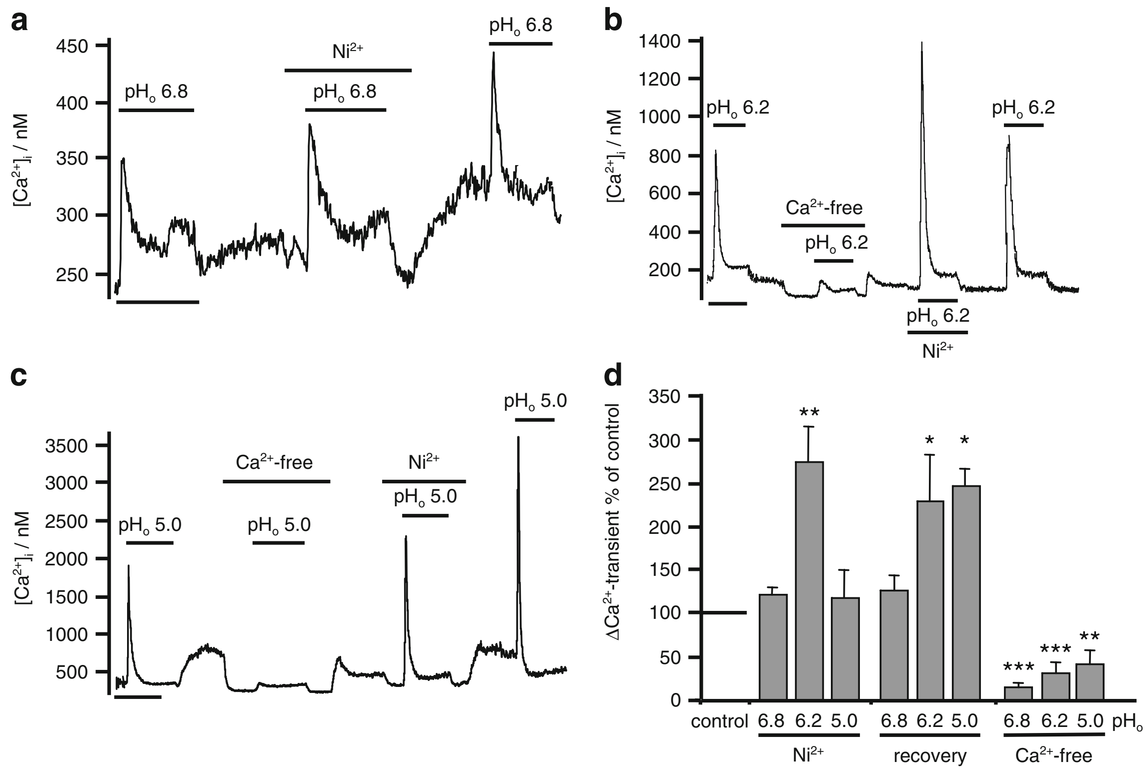

Fig. 5 Effects of Ni^{2+} on acid-evoked Ca^{2+} transients. Three different levels of external acidosis were used (pH_o 6.8, **a**; 6.2, **b**; 5.0, **c**). A control exposure to acidosis was followed by an exposure to acidosis in the presence of Ni^{2+} (2.5 mM) and finally by a second exposure to acidosis omitting Ni^{2+}. **a** Ca^{2+} transients evoked by pH_o 6.8 were unaffected by Ni^{2+}. **b** Ca^{2+} transients evoked by pH_o 6.2 were enhanced in the presence of Ni^{2+} and the post-Ni^{2+} (control) response to pH_o 6.2 was also augmented when compared to the first control response. **c** Ca^{2+} transients in response to pH_o 5.0 were unaffected by Ni^{2+} although the post-Ni^{2+} control response was again enhanced compared to the first control. **d** Summary of the effects of Ni^{2+} on Ca^{2+} transient response to acidosis. The data are presented as mean + SEM. Number for each experiment (n=6). Data on the effects of Ca^{2+}-free solutions upon acid-evoked Ca^{2+} transients are included for comparison. Statistical significance was assessed using Student's paired t test (*$p<0.05$; **$p<0.01$; ***$p<0.001$). Exposure periods in **a**–c are indicated by *horizontal bars*. *Time scale bars* in all recordings, 200 s

similar to findings seen during capsaicin application in the presence of Cd^{2+}.

Amiloride (100 μM), an inhibitor of ASICs, did not significantly attenuate the Ca^{2+} transients evoked by any of the three acid stimuli tested, nor did it affect the postamiloride control response to acidosis (Fig. 7).

CPZ (10 μM), an antagonist of capsaicin-mediated activation of TRPV1 [81], strongly inhibited the Ca^{2+} response to capsaicin (0.1–1 μM) as expected ($p<0.01$, n=6; see Supplementary material 1). In contrast, the Ca^{2+} transients evoked by three different acid stimuli were not attenuated by CPZ. Instead, there was a tendency for the Ca^{2+} transients in response to acidosis to be amplified slightly by the application of CPZ; this was significant at pH_o 6.2 (205±60%, n=6, $p<0.05$ when compared to first control). Ca^{2+} transients evoked by the final, control, exposure to pH_o 6.2 or 5.0 were also significantly larger than the first control Ca^{2+} transients (Fig. 8). Acid-evoked (pH_o 6.2) Ca^{2+} transients were greatly reduced by BCTC (1 μM) to 22±5% (n=12, $p<0.01$). AMG 9810 also substantially reduced initial Ca^{2+} transients to 15±3% (n=18, $p<0.001$; Fig. 9b, d) when compared to first control. Ca^{2+} transients evoked in response to lactic acidosis (15 mM Na-lactate, pH_o 6.2) were similarly reduced by both BCTC (to 15±4%, n=17, $p<0.001$) and by AMG 9810 (to 11±3%, n=8, $p<0.01$; Fig. 9c, d). For both BCTC and AMG 9810, the Ca^{2+}-transient response to acidosis remained reduced compared to initial controls after washout of the drug (Fig. 9d). A similar lack of rapid/full reversibility was also noted in the ability of both BCTC and AMG 9810 to antagonise responses to capsaicin (see Supplementary material 1).

Acidosis triggers a sustained Ca^{2+}-release from internal stores

The sustained rise in $[Ca^{2+}]_i$ evoked by hypercapnic acidosis pH_o 6.8 was 52±6 nM (n=17) and that evoked

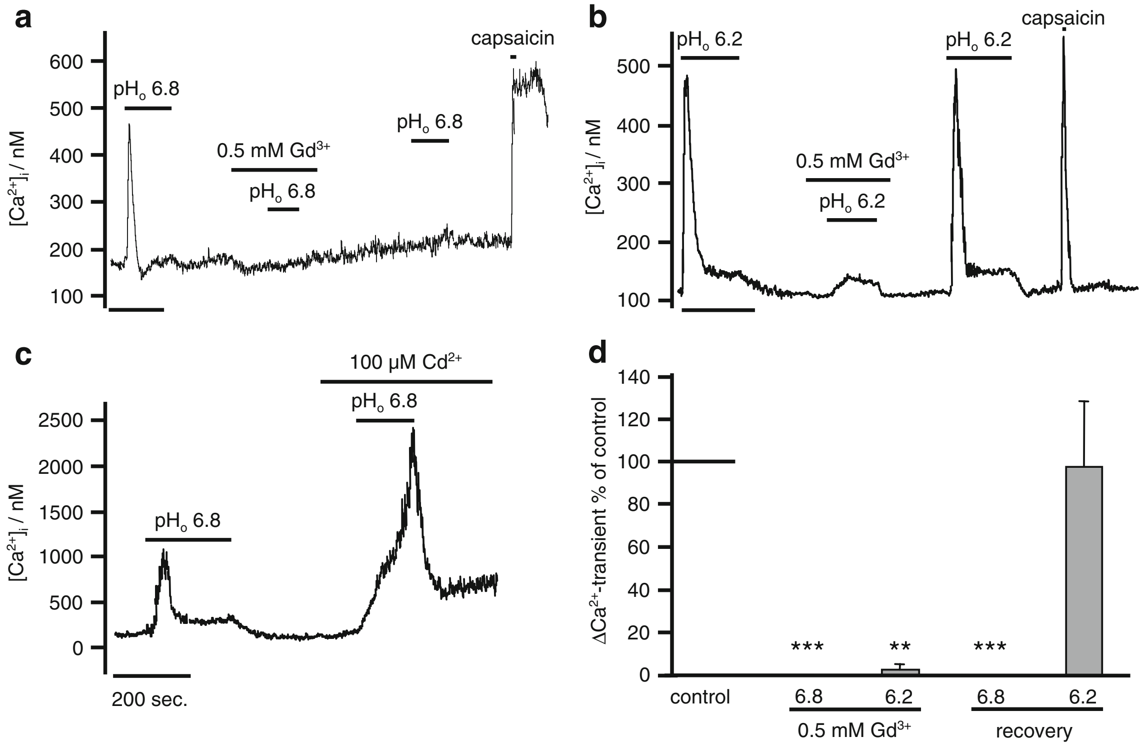

Fig. 6 Effects of Gd^{3+} and Cd^{2+} on acidosis-evoked Ca^{2+} transients. **a** Gd^{3+} (0.5 mM) completely inhibited Ca^{2+} transients as a response to pH_o 6.8. Ca^{2+} transients did not recover during a final exposure to pH_o 6.8; however, the final application of capsaicin (100 nM), to characterise the neurones, still evoked a rise in $[Ca^{2+}]_i$. **b** Ca^{2+} transients evoked by pH_o6.2 were significantly reduced by Gd^{3+} (0.5 mM) below 10% compared to control transients. Following Gd^{3+} removal, the Ca^{2+} response to pH_o 6.2 recovered fully. **c** In the presence of 100 µM Cd^{2+}, acidosis evoked a strong increase of Fura-2 fluorescence which only partially recovered. **d** Summary of the effects of Gd^{3+} on Ca^{2+} transients evoked by acidosis (normalised to the first control transient, arbitrarily set as 100%). Values are presented as mean + SEM (n=6 for each condition). Statistical significance was assessed using Student's paired t test (**p<0.01; ***p<0.001). Exposure periods are indicated by *horizontal bars*. *Time scale bars* in all recordings, 200 s

by a mixed acidosis pH_o 6.2 was 73±13 nM (n=13). There was no statistically significant difference between the sustained rise in $[Ca^{2+}]_i$ in response to these two stimuli (p=0.263). The sustained rise in $[Ca^{2+}]_i$ was not reduced by Ca^{2+}-free solutions (pH_o 6.8, 42±5 nM (n=10, p=0.223) and pH_o 6.2, 38±7 nM (n=7, p=0.097)).

In further experiments, we investigated whether this sustained Ca_o^{2+}-independent rise in $[Ca^{2+}]_i$ was due to acid-induced Ca^{2+} liberation from intracellular Ca^{2+} stores. Since we observed no differences between the sustained rises in $[Ca^{2+}]_i$ evoked either by pH_o 6.8 or pH_o 6.2, the following series of experiments were conducted using a single acid stimulus (hypercapnic acidosis pH_o 6.8). Depletion of endoplasmic reticulum (ER) stores using CPA (10 µM, a sarco-/endoplasmic reticulum Ca^{2+} ATPase (SERCA) inhibitor) significantly reduced the sustained rise in $[Ca^{2+}]_i$ to 24±12 nM (n=4, p<0.05; Fig. 10a, d). Application of caffeine (30 mM) to deplete ER stores also reduced the sustained rise in $[Ca^{2+}]_i$ to 11±2.4 nM (n=5, p<0.01; Fig. 10b, d). Depletion of mitochondrial Ca^{2+} stores by FCCP (1 µM) did not influence the sustained rise in $[Ca^{2+}]_i$ evoked by pH_o 6.8 (55±11 nM, n=6, p=0.235; Fig. 10c, d).

Effects of anoxia on the $[Ca^{2+}]_i$ response to acidosis

In vivo, the intense acidosis that accompanies ischaemia is primarily a consequence of the anaerobic generation of lactic acid due to a lack of oxygen delivery. Ischaemic acidosis is consequently invariably accompanied by anoxia. The following experiments were therefore conducted to investigate the effects of oxygen deprivation on the neuronal response to acidosis.

Exposure to anoxia plus hypercapnic acidosis (pH_o 6.8) evoked Ca^{2+} transients with a peak $\Delta[Ca^{2+}]_i$ of 353±214 nM (n=8; Fig. 11b). These Ca^{2+} transients were significantly larger (p<0.05, n=8) than those evoked by pH_o 6.8 alone (112±60 nM). Anoxia plus a mixed acidosis (pH_o 6.2) also evoked Ca^{2+} transients (498±25 nM, n=7) that were significantly (p<0.05, n=7) greater than those evoked by pH_o 6.2 alone (310±31 nM; Fig. 11a). Since the amplitude of the transient $[Ca^{2+}]_i$ response to acidosis

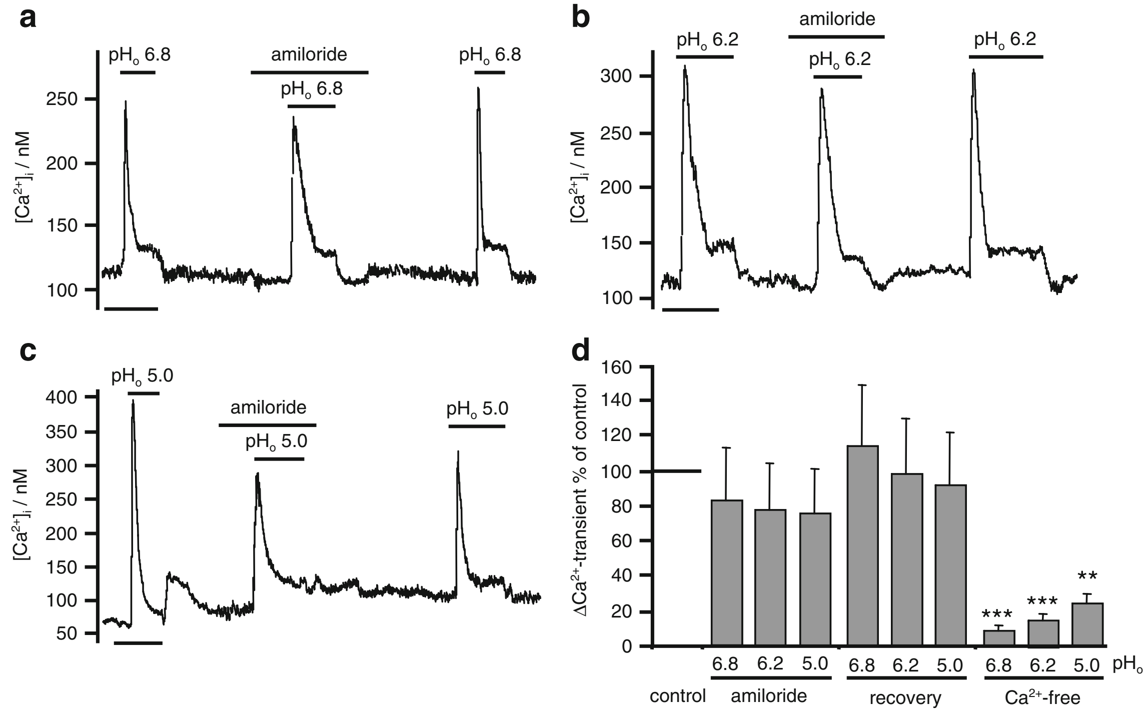

Fig. 7 Sensitivity of acidosis-evoked Ca^{2+}-influx to amiloride. **a**–**c** The effects of amiloride (100 μM) on acid-evoked Ca^{2+} transients was tested at three different pH_o values (5.0, 6.2, 6.8). Note that the intrinsic fluorescence of amiloride causes only a very small baseline shift indicating negligible interference with Fura-2 fluorescence measurements. **d** Summary of the effects of amiloride on acid-evoked Ca^{2+} transients. Data are normalised to the initial control responses (arbitrarily set as 100%). Note that although there is a tendency for amiloride to reduce the effect of acidosis by 10–20%, this failed to reach statistical significance. The effects of Ca^{2+}-free solutions on the acid-evoked Ca^{2+} transients are included for comparison. Statistical significance was assessed using Student's paired *t* test (**$p<0.01$; ***$p<0.001$). Exposure periods are indicated by *horizontal bars*. Each experimental group includes six independent recordings. *Time scale bars* in all recordings, 200 s

tended to vary widely between cells, these data were normalised to the Ca^{2+} transient evoked under normoxic conditions (set as 100%) and are presented in Fig. 11e. In addition to increasing Ca^{2+}-transient amplitude, anoxia also appeared to slow the recovery (rate of decline) of the $[Ca^{2+}]_i$ transient. Under control conditions, recovery rates (measured over the range 200–250 nM) were 3.7±0.5 nM/s at pH_o 6.8 and 4.3±0.8 nM/s at pH_o 6.2. In anoxia, these rates were slowed to 2.2±0.5 nM/s ($p<0.05$, $n=8$) at pH_o 6.8 and 1.7±0.6 nM/s ($n=8$, $p<0.01$) at pH_o 6.2. Ca^{2+} transients generated in response to anoxic–acidosis were either completely prevented or were significantly reduced in Ca^{2+}-free medium (pH_o 6.8, $\Delta[Ca^{2+}]_i=11\pm4$ nM, $n=6$, $p<0.05$; pH_o 6.2, $\Delta[Ca^{2+}]_i=79\pm14$ nM, $n=5$, $p<0.05$; Fig. 11d, f).

For comparison, we also investigated the effects of anoxia upon the Ca^{2+} transients evoked by capsaicin (100 nM for 10 s). Capsaicin-evoked Ca^{2+} transients were also amplified under anoxic conditions to 140±6% of control ($p<0.01$, $n=6$; Fig. 11c, e). Moreover, the recovery rates of these Ca^{2+} transients were significantly slowed from 9±1.6 nM/s under normoxia to 3.4±0.8 nM/s during anoxic conditions ($n=6$, $p<0.01$).

The sustained rise in $[Ca^{2+}]_i$ induced by anoxia and acidosis was also significantly greater than that evoked by acidosis alone. At pH_o 6.8 in anoxia, the sustained rise in $[Ca^{2+}]_i$ was 84±9 nM ($n=13$) vs. 52±6 nM ($n=17$) in pH_o 6.8 alone ($p<0.01$). Similarly at pH_o 6.2 in anoxia, the sustained rise in $[Ca^{2+}]_i$ was 104±25 nM ($n=12$) vs. 73±13 nM ($n=13$) in pH_o 6.2 alone ($p<0.05$).

Ca^{2+} responses to a combination of anoxia, acidosis and aglycaemia

In addition to anoxia, under ischaemic conditions, there may also be consumption of exogenous glucose. So, we also investigated the effects of combining acidosis and anoxia with aglycaemia. In the following experiments combining extracellular acidosis (pH_o 6.8 or 6.2) with anoxia and aglycaemia (aaa 6.8 and aaa 6.2) resulted in a rapid transient increase in $[Ca^{2+}]_i$ followed by a sustained rise in $[Ca^{2+}]_i$ in the majority (65%) of neurones (see, e.g. Fig. 12a, e). In a small subpopulation of neurones (30%), however, the initial Ca^{2+} transient was absent or very small and only a sustained rise in $[Ca^{2+}]_i$ was seen (e.g. Fig. 12b).

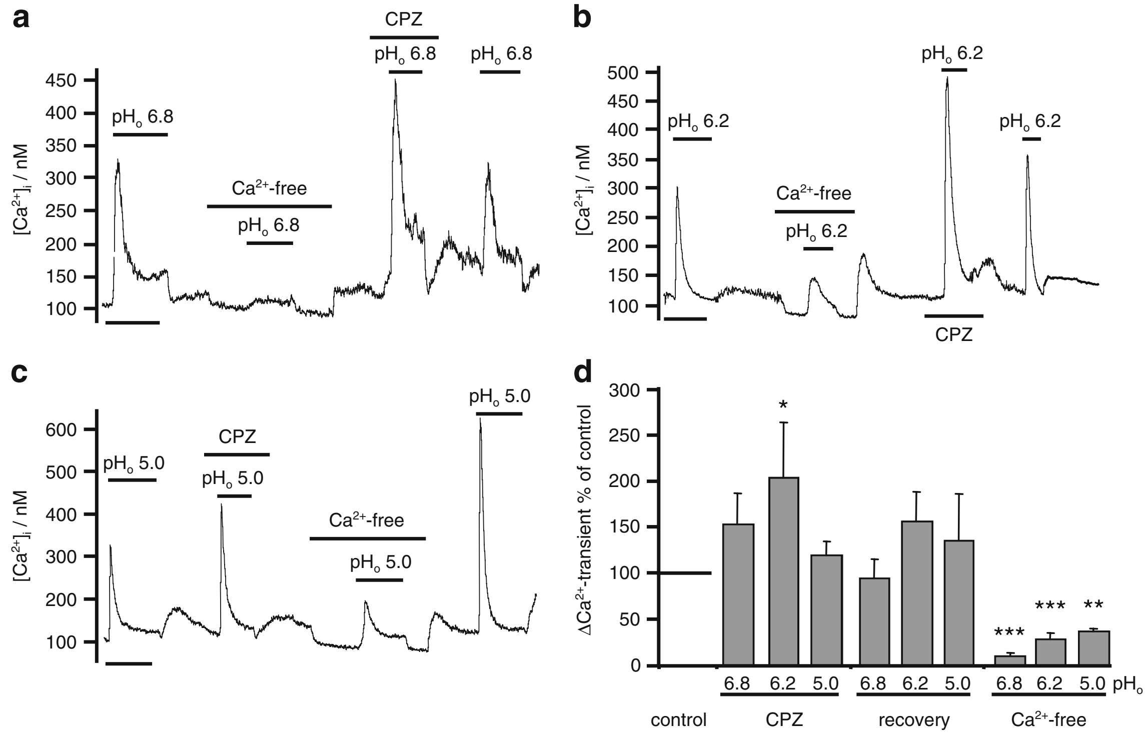

Fig. 8 a–c Effects of CPZ on acidosis-evoked Ca^{2+} transients. Experiments were conducted using three different levels of acidosis pH 6.8 (**a**), pH 6.2 (**b**) and pH 5.0 (**c**). Note that in contrast to its effects on capsaicin-evoked Ca^{2+} transients, capsazepine failed to inhibit acid-evoked Ca^{2+} transients. **d** Mean data from experiments in **a**–**c**. Ca^{2+} transients were normalised to control Ca^{2+} transients (set to 100%). Note that instead of inhibiting the response to acidosis, CPZ amplified the response to pH_o 6.2. The effects of removal of extracellular Ca^{2+} on the acid-evoked Ca^{2+} response are included for comparison. Exposure periods are indicated by *horizontal bars*. Number of each experimental condition: n=6. Statistical significance was assessed using Student's paired t test (*p<0.05; **p<0.01; ***p<0.001). *Time scale bars* in all other recordings, 200 s

By comparison, the responses to anoxia alone or aglycaemia alone consisted only of a monophasic sustained increase in $[Ca^{2+}]_i$ (see Fig. 12a, b, e, f). The sustained rise in $[Ca^{2+}]_i$ evoked by the combination of anoxia, acidosis and aglycaemia was found to be larger than that evoked by any of these stimuli in isolation (see Fig. 12g, h; although the difference between pH_o 6.8 and pH_o 6.8 + anoxia and aglycaemia just failed to reach statistical significance). This suggests that the effects of these stimuli on sustained $[Ca^{2+}]_i$ are additive (see "Discussion" section).

As noted above, Ca^{2+} transients were only observed under acid conditions and not with anoxia or aglycaemia alone. The amplitude of these acid-evoked $[Ca^{2+}]_i$ transients were, however, augmented by both anoxia and the combination of anoxia and aglycaemia with the effects of anoxia and aglycaemia being larger than the effects of anoxia alone (see Fig. 13). We also noted that the recovery rates of Ca^{2+} transients evoked by aaa pH_o 6.8 (1.9±0.5 nM/s, n=26) and aaa pH_o 6.2 (2.5±0.4 nM/s, n=16) were again significantly reduced when compared to pH_o 6.8 and pH_o 6.2 alone (p<0.05), but were not different to the recovery rates of Ca^{2+} transients evoked by anoxia pH_o 6.2 or anoxia pH_o 6.8.

Identification of Ca^{2+}-influx pathways activated by aaa pH_o 6.8

As previously observed for acidosis alone, the initial Ca^{2+} transient in response to aaa was greatly inhibited in Ca^{2+}-free media whereas the sustained elevation in $[Ca^{2+}]_i$ was independent of external Ca^{2+} (see Fig. 14). Having determined that the initial Ca^{2+} transients in response to the combination of acidosis, anoxia and aglycaemia is dependent upon Ca^{2+} influx, we next sought to identify the ion channels responsible for this Ca^{2+} influx. Neurones were exposed to aaa pH_o 6.8 alone (control) and then to aaa 6.8 in the presence of amiloride, Ni^{2+}, capsazepine, Gd^{3+} and then to aaa 6.8 again (second control). The amplitudes of the resulting Ca^{2+} transients were normalised to the first control response (arbitrarily set as 100%). Amiloride (100 µM) reduced Ca^{2+} transients to 50±8% (n=6, p< 0.01) compared to control (Fig. 15a, e). Ni^{2+} (2.5 mM) had no significant effect on Ca^{2+} transients (81±21%, n=5, p=0.413; Fig. 15b, e). Capsazepine (10 µM) also had no significant effect upon the Ca^{2+} transient (86±7% compared to control, n=5, p=0.1; Fig. 15c, e). In the presence of Gd^{3+} (1 mM), Ca^{2+} transients evoked by aaa pH_o 6.8

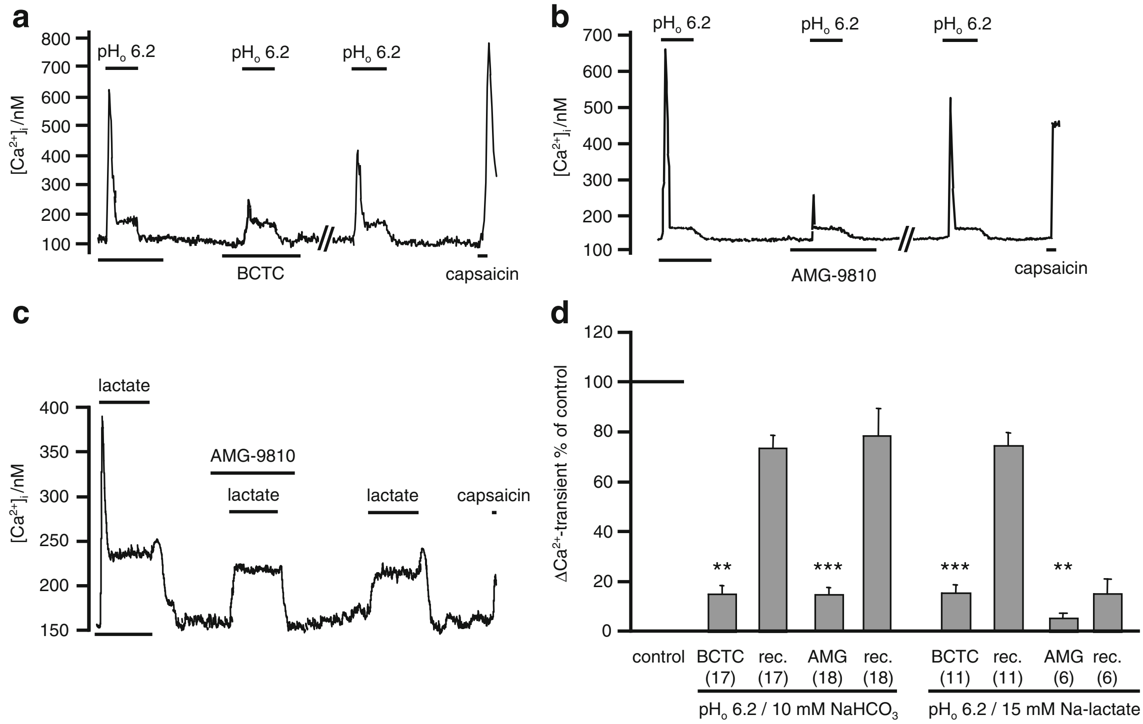

Fig. 9 Effects of BCTC and AMG 9810 (AMG) on acid (pH_o 6.2) evoked Ca^{2+} transients. **a**, **d** BCTC (1 μM) reduced Ca^{2+} transients evoked by a mixed acidosis (pH_o 6.2, 20% CO_2) to 22%. The effects of BCTC were only partially reversible. **b**, **d** AMG 9810 (AMG, 1 μM) reduced mixed acidosis-evoked Ca^{2+} transients to 15% when compared to first control acidic stimulus. The effects of AMG were also only partially reversible. **c**, **d** BCTC and AMG 9810 significantly inhibited Ca^{2+} transients evoked by a lactic acidosis (pH_o 6.2, 20% CO_2 15 mM Na-lactate). Breaks in recordings (**a**–**c**) before the second control acidic stimulus were approximately 10 min (to try to facilitate reversal of effects of BCTC and AMG 9810). *Time scale bars* in all recordings, 200 s. Statistical significance was assessed using Student's paired *t* test (**$p<0.01$; ***$p<0.001$, number of experiments are in *parenthesis*). *rec.* recovery, i.e. second postdrug control acid stimulus; lactate=15 mM Na-lactate

were reduced to 45±9% ($n=6$, $p<0.05$; Fig. 15d, e). BCTC (1 μM) and AMG 9810 also inhibited Ca^{2+} transients evoked by aaa pH_o 6.2 (Fig. 16a, b, d). Ca^{2+} transients were reduced to 9±6% ($n=6$, $p<0.001$) by BCTC and to 11±8% ($n=6$, $p<0.001$) by AMG 9810, respectively. Ca^{2+} transients evoked by lactic acidosis in the presence of anoxia and aglycaemia (20% CO_2 in 15 mM Na-lactate) were similarly reduced by AMG 9810 to 11±5% ($n=6$, $p<0.001$; Fig. 16c, d). The effects of BCTC and AMG 9810 were again largely irreversible within the time frame of these experiments (Fig. 16a–c). Thus, the Ca^{2+} transient evoked by aaa was strongly inhibited by BCTC and AMG 9810 (although not completely abolished) was roughly halved by amiloride and Gd^{3+} but was unaffected by Ni^{2+} or capsazepine.

Discussion

In this study, we have investigated the effects of acidosis, anoxia and aglycaemia on $[Ca^{2+}]_i$ in sensory neurones. Acidosis is considered to be one of the primary stimuli responsible for sensory neurone excitation in ischaemia [68]. It also plays a pivotal role in triggering neuronal release of CGRP [25, 73, 113]. The secretion CGRP in response to a number of stimuli, including acidosis, is critically dependent upon Ca^{2+} signalling [23, 28, 56].

In the first part of this study, we investigated the effects of acidosis alone on intracellular $[Ca^{2+}]_i$ in small capsaicin-sensitive neurones arising from dorsal root ganglia as these are thought to be responsible for sensing ischaemic conditions [17, 68, 88]. In the second part of the study, we have compounded the effects of acidosis with anoxia and aglycaemia since these conditions not only accompany ischaemia but can have profound effects upon Ca^{2+} regulation in sensory neurones [34, 55, 69, 75].

Effects of acidosis alone on $[Ca^{2+}]_i$ in sensory neurones

We have employed four different levels and types of acidosis in this study: a relatively mild hypercapnic acidosis (pH 6.8; 20% CO_2 and normal bicarbonate) representative of the early stages of ischaemia in the heart, a more severe mixed acidosis (pH 6.2; 20% CO_2 and reduced bicarbonate) and an equivalent mixed acidosis including 15 mM Na-lactate representative of the latter stages of ischaemia and a

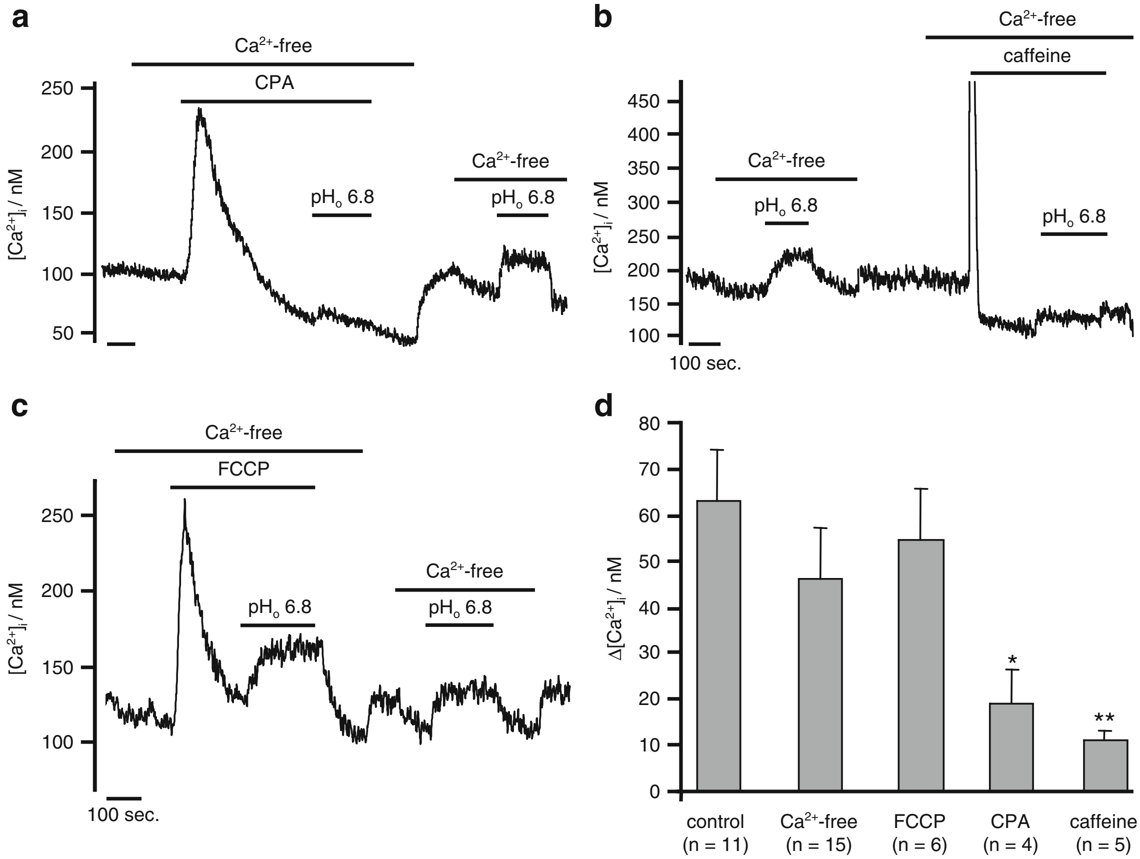

Fig. 10 ER Ca^{2+} stores contribute to the acidosis evoked sustained rise in $[Ca^{2+}]_i$. **a**–**c** In Ca^{2+}-free media acidosis (pH_o 6.8) evoked a sustained rise in $[Ca^{2+}]_i$. **a** Effects of ER store depletion with CPA (10 μM) on the acid evoked rise in $[Ca^{2+}]_i$. **b** Effects of ER store depletion with caffeine (30 mM). **c** Effects of mitochondrial Ca^{2+}-store depletion with the uncoupler FCCP (1 μM). **d** Summary of effects of CPA, caffeine and FCCP on the acidosis evoked rise in $[Ca^{2+}]_i$ in Ca^{2+}-free media. Statistical significance was assessed using Student's paired *t* test (**$p<0.01$; *$p<0.05$ compared to acidic exposure in Ca^{2+}-free solution). Exposure periods are indicated by *horizontal bars*. *Time scale bars*, 200 s

very severe acidosis (pH_o5.0) representative of the stimuli frequently used to activate acid sensitive cation channels in vitro [10, 52, 110]. All four acid stimuli evoked a biphasic elevation of $[Ca^{2+}]_i$ in the majority of neurones investigated. The initial phase was characterised by a Ca^{2+} transient occurring within the first minute of exposure to acidosis. This initial transient was chiefly dependent on external Ca^{2+}. The Ca^{2+} transient was then followed by a sustained elevation of $[Ca^{2+}]_i$. This second sustained phase of the $[Ca^{2+}]_i$ response was not depended upon Ca^{2+} influx. We will first address possible mechanisms for these Ca^{2+} signalling events.

Pharmacological identification of Ca^{2+} influx pathways

The most likely mechanisms for acid-evoked Ca^{2+} influx in neurones are through (a) ASIC1a channels [101, 102, 110], (b) TRPV1 (or capsaicin) receptors [17, 89] and (c) voltage-gated Ca^{2+} channels secondary to acid-evoked membrane depolarisation [15, 40, 87]. In order to discriminate between these entry pathways, we needed to find suitable pharmacological tools.

ASIC channels are widely reported to be inhibited by amiloride [106] although this is not entirely selective as amiloride may also inhibit T-type voltage-gated Ca^{2+} channels [86, 95]. Recent evidence also indicates that under moderate acidosis (pH 7.0), amiloride may activate ASIC3 leading to sustained inward currents [108].

Although there are several different types of voltage-gated Ca^{2+} channels in sensory neurones [3, 4], there are a number of divalent cations that can be used to inhibit all high voltage-activated channels (cadmium) and both high and low voltage-activated channels (nickel) [9, 13, 62, 64, 71, 74, 95]. Using high potassium solutions to depolarise, we confirmed that 100 μM Cd^{2+} substantially blocked and 2.5 mM Ni^{2+} fully blocked voltage-gated Ca^{2+} entry. We next tested the effects of these cations on capsaicin evoked Ca^{2+} influx to see if they could be used to discriminate between TRPV1 and voltage-gated Ca^{2+} entry. Capsaicin-induced Ca^{2+} transients were not inhibited by either Ni^{2+} or

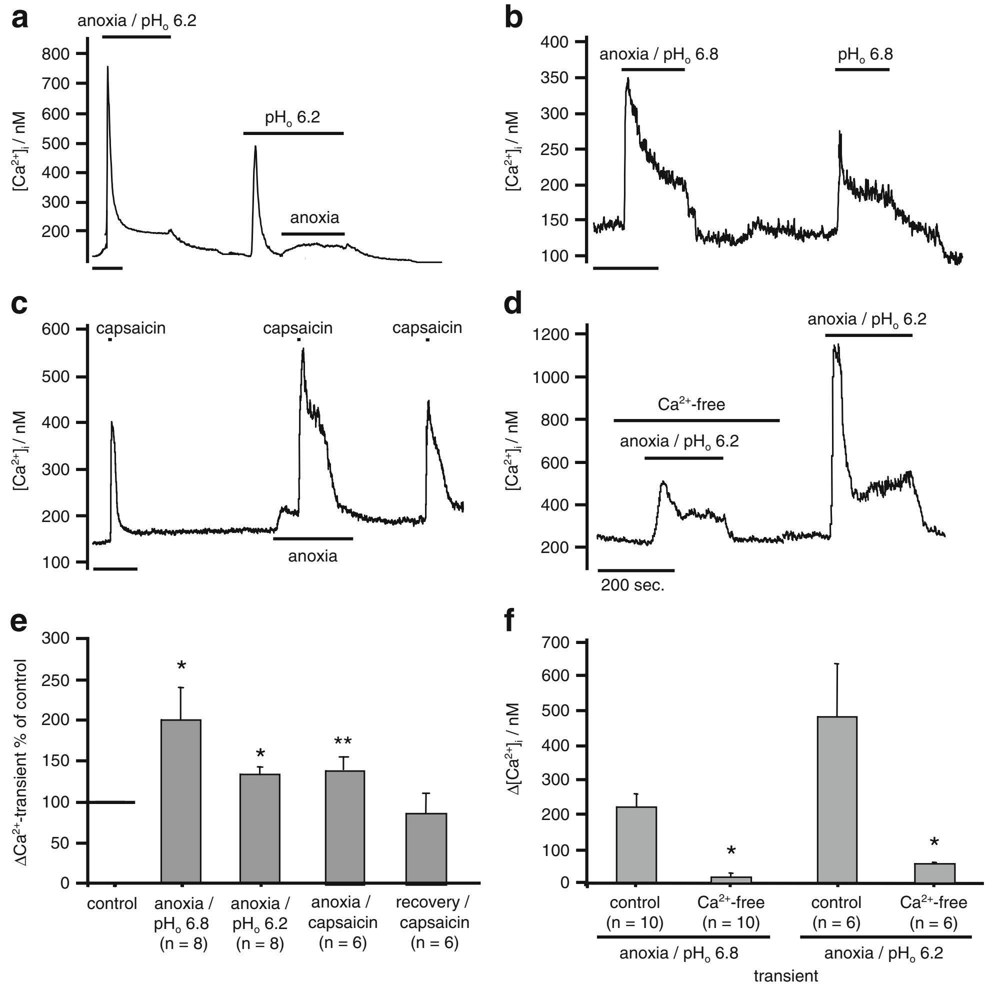

Fig. 11 Effects of anoxia on acid and capsaicin-evoked Ca^{2+} signalling. **a**, **b** Effects of anoxia on acid (pH$_o$ 6.8 and pH$_o$ 6.2) evoked Ca^{2+} responses. **c** Effects of anoxia on Ca^{2+} response to capsaicin (100 nM for 10 s). **d** Effects of removal of extracellular Ca^{2+} on Ca^{2+} response to acidic anoxia. **e** Summary of the effects of anoxia on the initial Ca^{2+} transient generated in response to acidosis and capsaicin. Data are normalised to the control response (in absence of anoxia) which is arbitrarily set to 100%. Values are means + SEM. **f** Summary of the effects of Ca^{2+}-free media on the initial $[Ca^{2+}]_i$ transient generated in response to acidic anoxia. Data are means + SEM. Statistical significance (in **e** and **f**) was assessed using Student's paired *t* test (**p<0.01; *p<0.05). Numbers of experiments are given in *parenthesis*. Exposure periods (in **a**–**d**) are indicated by *horizontal bars*. *Time scale bars*, 200 s

Cd^{2+}; indeed, the effects of capsaicin appeared to be potentiated. In particular, exposure to capsaicin in the presence of Cd^{2+} led to a substantial and mostly irreversible increase in the Fura-2 fluorescence ratio. We suggest that this is probably due to Cd^{2+} entry through TRPV1 and subsequent binding of Cd^{2+} to Fura-2. Cd^{2+} binding to Fura-2 has similar effects on its fluorescence to those of Ca^{2+} binding but Fura-2 has a much greater affinity for Cd^{2+} than for Ca^{2+} [36]. Ni^{2+} ions can also bind to Fura-2 but when they do so, they quench fluorescence. No fluorescence quenching was observed during exposure to capsaicin in the presence of Ni^{2+} suggesting that Ni^{2+} does not pass through TRPV1 to any significant extent. Ni^{2+} was also ineffective in inhibiting capsaicin-evoked Mn^{2+} entry (TRPV1 channels are permeable to Mn^{2+} [66]), whereas it fully blocked voltage-gated Mn^{2+} entry. Mn^{2+} quenching of Fura-2 fluorescence in the presence of Ni^{2+} may therefore also serve as an indicator of TRPV1 activation. One possible problem with the use of Ni^{2+} is that it appeared to slightly potentiate the effects of capsaicin. Sensitisation of TRPV1 channels by other external cations, Na^+ and Mg^{2+}, has been previously described [1]. Despite this sensitisation, the effects of Ni^{2+} and Cd^{2+} should permit discrimination between voltage-gated and TRPV1-mediated Ca^{2+} influx.

The TRPV1 antagonist capsazepine was, as expected, highly efficient in blocking the effects of capsaicin [31, 51, 53]. Whether it can also block acid-evoked activation of TRPV1 is, however, uncertain (see below). We therefore sought other blockers of Ca^{2+} entry through TRPV1. Gadolinium (Gd^{3+}) is a small lanthanide that blocks various types of calcium channels at submillimolar concentrations [7, 14, 49, 62]. Gd^{3+} has been reported to activate and sensitise TRPV1 channels at low concentrations, but at higher concentrations (>300 μM), it inhibits capsaicin-evoked membrane currents [1, 92]. In the present study, Gd^{3+} inhibited both voltage-activated Ca^{2+} entry and capsaicin-evoked Ca^{2+} influx, but we could only inhibit capsaicin-evoked Ca^{2+} transients with Gd^{3+} concentrations of 500 μM and above. Two newer TRPV1 antagonists BCTC and AMG 9810 with reported ability to block proton activation of TRPV1 were also tested [27, 93]. These produced a profound block of capsaicin-evoked Ca^{2+} transients that was largely irreversible.

Fig. 12 Effects of combining anoxia, aglycaemia and acidosis on $[Ca^{2+}]_i$. **a**–**f** Acidic stimuli (pH_o 6.8 or pH_o 6.2) together with anoxia and acidosis (*aaa*) were applied simultaneously and compared with aglycaemia (**a**, **b**), an equivalent acidosis (**c**, **d**) or anoxia (**e**, **f**) alone. In this series of experiments, the order of application of stimuli was randomised to exclude any systematic bias due to sensitisation or desensitisation. *Time scale bars* are 200 s. **g**, **h** Summary data showing comparison of effects of combined anoxia, aglycaemia and acidosis (**g** pH_o 6.8, **h** pH_o 6.2) with each individual stimulus in isolation on the sustained elevation of $[Ca^{2+}]_i$. Data are means + SEM. Statistical significance was assessed by Student's paired *t* test (*$p<0.05$; **$p<0.01$); the number of experiments are given in *parenthesis*

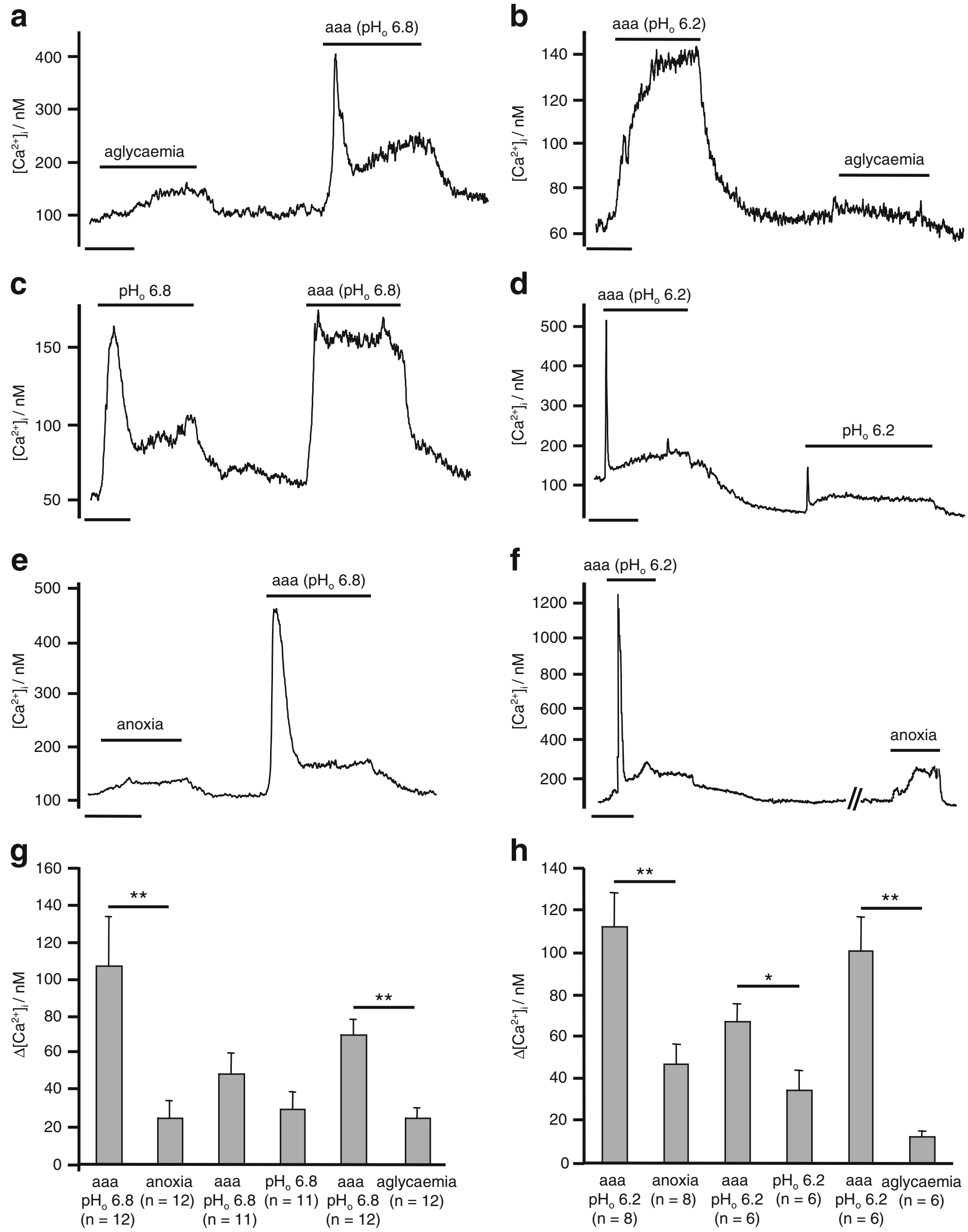

Acid-evoked Ca^{2+} influx pathways

Protons activate strong inward sodium currents in DRG neurones which have both transient and sustained components [10]. These currents are mediated mainly by ASIC3, a proton-sensitive cation channel [29, 57, 67, 77]. ASICs are thought to play a key role in transmitting ischaemic pain. They are directly activated by extracellular acidosis which relieves channel blockade by Ca^{2+} ions through the protonation of the Ca^{2+}-binding sides [41, 42, 78]. The ion selectivity of these channels is not restricted to Na^+; ASIC1a is also permeable to Ca^{2+} [19, 99, 105, 110] and contributes to the Ca^{2+} overload in neurones of ischaemic brain [107]. In the present study, amiloride was administered to evaluate the contribution of ASICs to the acid-evoked Ca^{2+} transients [10, 18, 99]. Surprisingly although there was a general tendency for amiloride to reduce the acid-evoked Ca^{2+} transient at all pH values tested, this effect did not reach statistical significance and robust Ca^{2+} transients invariably remained. Thus, although we cannot completely exclude a minor role for ASICs in mediating some of the acid-evoked Ca^{2+} influx, they are clearly not the main cause.

We also tested the effects of Ni^{2+} and Cd^{2+} on the Ca^{2+} response to acidosis. Both of these agents failed to inhibit the acid-evoked Ca^{2+} transient. Ni^{2+} also failed to inhibit acid-evoked Mn^{2+} influx (see Fig. 4c). These data indicate

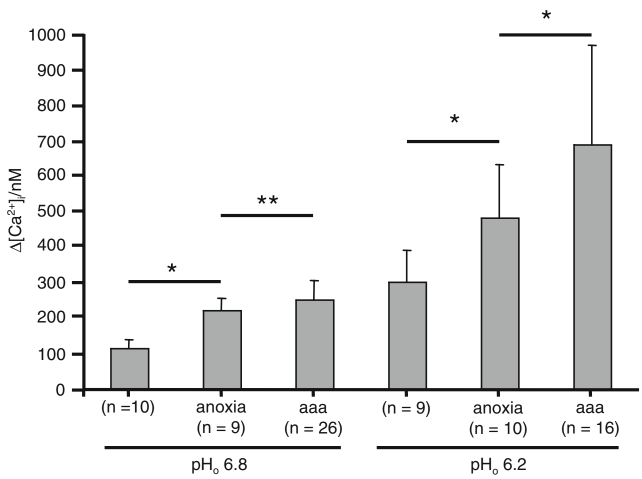

Fig. 13 Comparison of Ca^{2+}-transient amplitude in response to acidosis, anoxic acidosis and anoxic aglycaemic acidosis. Studies were conducted at two levels of acidosis pH_o 6.8 and pH_o 6.2. Data are mean + SEM with *n* in *parenthesis*. Statistical comparisons, indicated by *bars*, were conducted using Mann–Whitney *U* test ($*p<0.05$; $**p<0.01$)

that the Ca^{2+} transient is not primarily a consequence of membrane depolarisation followed by voltage-gated Ca^{2+} entry and point instead to another acid-activated cation channel. The fact that acid evoked a sustained rise in Fura-2 fluorescence ratio in the presence of Cd^{2+} suggests that this channel is also permeable to Cd^{2+}. Acid-evoked Ca^{2+} transients were, however, completely blocked by 500 µM Gd^{3+} and blocked by 85–90% by BCTC and AMG 9810. These characteristics, resistance/sensitisation by Ni^{2+}, permeability to Mn^{2+} and Cd^{2+}, block by high levels of Gd^{3+} and block by BCTC and AMG 9810 are identical to those of TRPV1 as described above. We also noted a positive correlation between the amplitudes of acidosis- and capsaicin-evoked Ca^{2+} transients (see Fig. 2).

Although the above data point to TRPV1 as being the main pathway for Ca^{2+} entry, it was notable that capsazepine failed to inhibit the acid-evoked Ca^{2+} transients. There are conflicting reports in the literature regarding the capsazepine sensitivity of both proton-activated inward currents in rat sensory neurones and the cloned rat TRPV1 channel. Tominaga and Tominaga originally reported that 10 µM capsazepine inhibited proton activated currents through cloned rat TRPV1 channels by approximately 80% [89], but others have subsequently found no effect at concentrations up to 30 µM [61, 65]. Similarly in rat sensory neurones, there are some reports that the sustained proton-activated currents are inhibited by capsazepine [52] and others which show no effect of capsazepine on proton-evoked currents or ion fluxes [11, 98]. Absence of effects of capsazepine upon proton activation of TRPV1 is not surprising since the capsaicin/capsazepine binding site and proton binding site are at different locations (capsaicin binds an intracellular domain [45] whereas protons bind to an extracellular domain [43]). The lack of consistency with respect to the effects of capsazepine on proton-activated TRPV1 currents in rat is, however, puzzling. Nevertheless, as there is clear precedent for lack of effect of capsazepine

Fig. 14 **a**, **b** Effects of removal of extracellular Ca^{2+} upon $[Ca^{2+}]_i$ responses to combined acidosis (**a** pH_o 6.8, **b** pH_o 6.2) anoxia and aglycaemia. The initial Ca^{2+} transient in **b** was out of scale. **c**, **d** Summary of the effects of Ca^{2+} removal on both the $[Ca^{2+}]_i$ transient and the sustained rise in $[Ca^{2+}]_i$ in response to combined acidosis anoxia and aglycaemia. Statistical significance was assessed by Student's paired *t* test ($*p<0.05$; $**p<0.01$). Numbers of experiments are given in *parentheses*. Exposure periods are indicated by *horizontal bars*. *Time scale bars*, 100 s

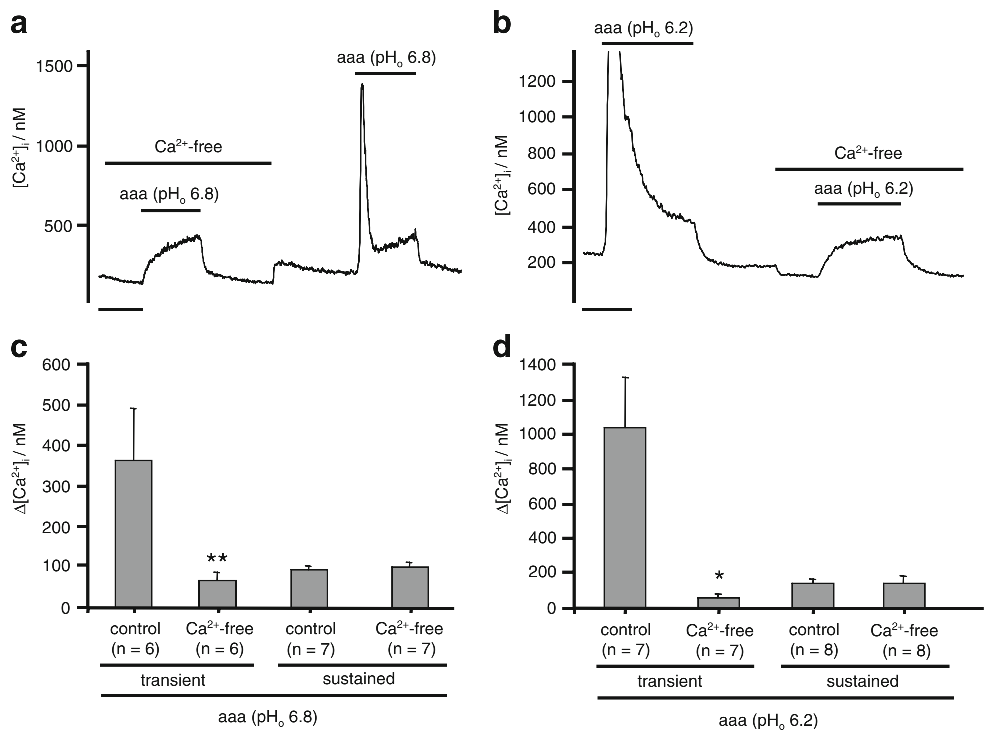

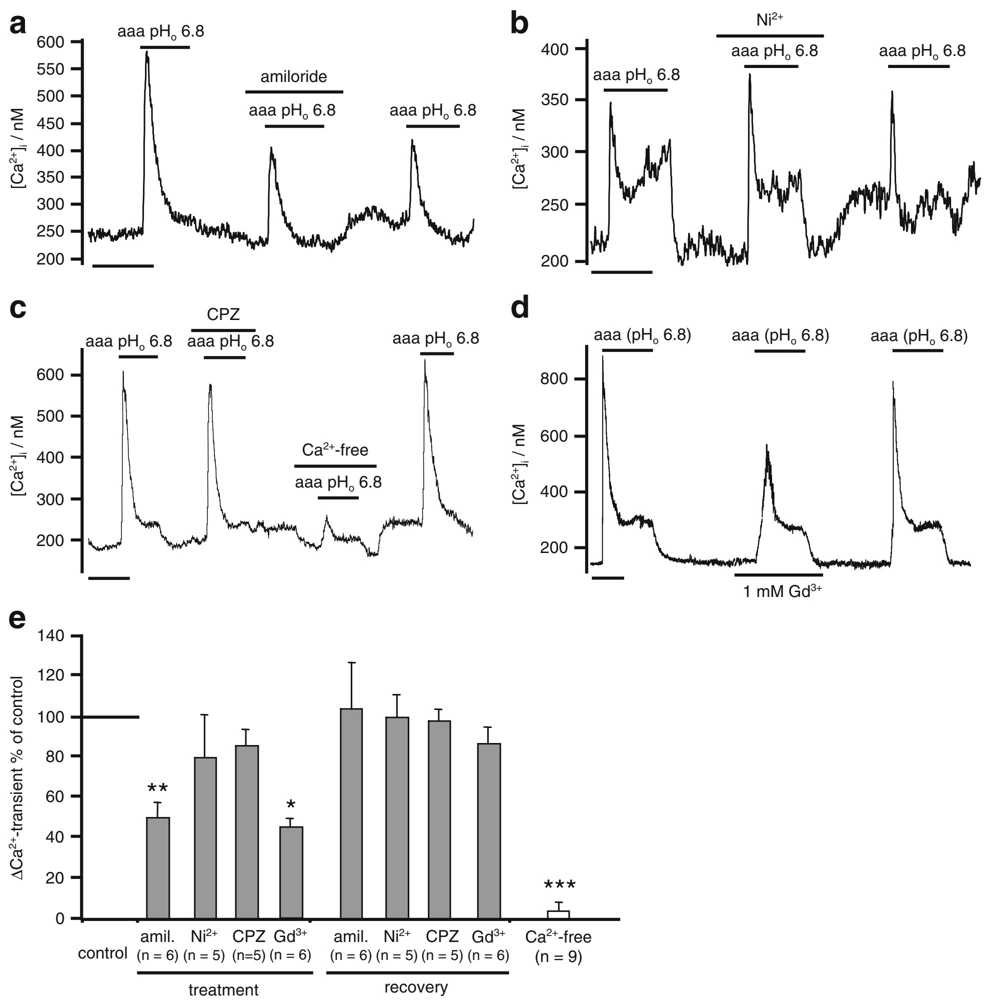

Fig. 15 Identification of calcium entry pathways activated in acidic (pH_o 6.8) anoxic aglycaemia. **a** Effects of the ASIC inhibitor amiloride (100 μM). **b** Effects of the voltage-gated Ca^{2+}-channel inhibitor Ni^{2+} (2.5 mM). **c** Effects of the capsaicin antagonist capsazepine (*CPZ*; 10 μM). **d** Effects of the trivalent cation Gd^{3+}. **e** Summary of effects of amiloride, Ni^{2+} capsazepine and Gd^{3+} on Ca^{2+}-transient amplitude in response to acidic anoxic aglycaemia. Data are normalised to the control transient recorded in the absence of drug (set to 100%). Statistical significance was assessed using Student's paired *t* test (*$p<0.05$; **$p<0.01$; ***$p<0.001$). Exposure periods are indicated by *horizontal bars*. *Time scale bars* are 200 s

on proton activation of rat TRPV1 and given the strong inhibitory effects of two other TRPV1 antagonists, the failure of capsazepine to antagonise the proton-activated Ca^{2+} influx cannot be considered to exclude a role for TRPV1.

In summary, the primary route for acid-evoked Ca^{2+} influx is via TRPV1. We cannot entirely exclude some contributory role for parallel voltage-gated Ca^{2+} entry (secondary to membrane depolarisation) since possible sensitisation of TRPV1 by Ni^{2+} may obscure any minor contribution from voltage-gated Ca^{2+} channels. The lack of any apparent major role for ASIC channels may seem surprising, but it should be noted that many of these channels inactivate very rapidly [10, 42, 78] so any Ca^{2+} influx will be short-lived and could easily be obscured by the subsequent Ca^{2+} influx through TRPV1.

Ca^{2+} liberation from internal stores during external acidosis

During exposure to acidosis, there is also a rise in $[Ca^{2+}]_i$ that is independent from Ca_o^{2+}. The sustained nature of this $[Ca^{2+}]_i$ rise suggests a change in the equilibrium between Ca^{2+} fluxes into and out of the cytosol (note that a discrete Ca^{2+}-release event alone, for example, displacement of Ca^{2+} from internal buffers by H^+, would be expected to only result in a transient increase in $[Ca^{2+}]_i$ as the Ca^{2+} released is subsequently extruded). We have not investigated the cause of this sustained rise in $[Ca^{2+}]_i$ in any detail, but we have observed that ER Ca^{2+}-store depletion using either caffeine or CPA reduces this acid induced rise in $[Ca^{2+}]_i$. One possible explanation therefore is that intracellular acidosis causes a sustained increase in Ca^{2+} leak from the ER.

Whilst a number of studies indicate that a direct effect of intracellular acidosis is to inhibit the ryanodine receptor [6, 84], there is another indirect pathway whereby Ca^{2+} release from internal stores may be triggered by the activation of proton-sensing G protein-coupled receptors [39, 54, 90]. These receptors have recently been described in approximately 75% of small nociceptive DRG neurones in which they are colocalised with ASICs [38]. In addition to the possibility of enhanced Ca^{2+} release, acidosis may also reduce Ca^{2+} reuptake into the ER by inhibiting SERCA. Moreover, our observation that a small (acid evoked)

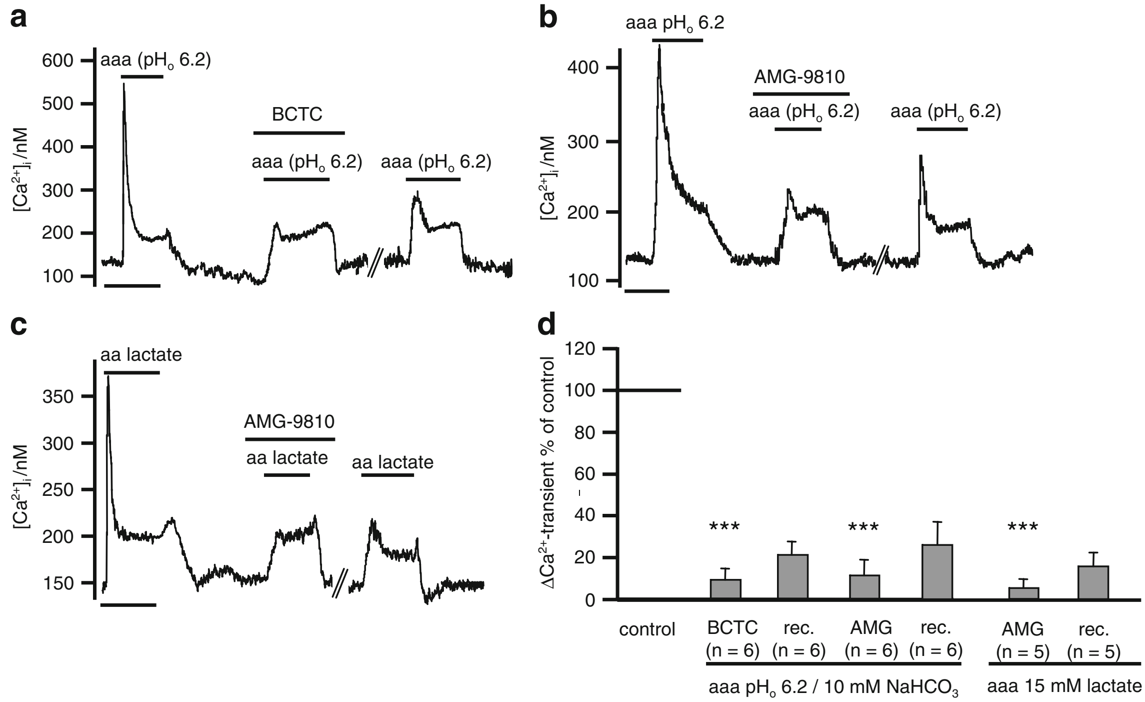

Fig. 16 Effects of the TRPV1 inhibitors BCTC (1 μM) or AMG 9810 (1 μM, AMG) on Ca^{2+} transients evoked by acidosis, anoxia and aglycaemia (*aaa*). **a**, **b** Mixed acidosis (20% CO_2 in pH 6.2). **c** Mixed acidosis with lactate (20% CO_2, 15 mM Na-lactate, pH 6.2). **d** Comparison of aaa evoked Ca^{2+}-transient amplitudes in the presence of BCTC and AMG 9810. Ca^{2+}-transient amplitude is expressed as a percentage of the first control response to aaa. Note that both inhibitors reduced initial Ca^{2+} transients significantly (for both types of acidosis) but did not completely abolish them. Interruptions in the recordings between the application of the inhibitor and the second control were approximately 10 min (to allow for washout of AMG 9810 or BCTC). Despite this wash period Ca^{2+} transients did not fully recover following removal of either BCTC or AMG 9810. Data are means + SEM; statistical significance was assessed using Student's paired *t* test (***$p<0.001$). Exposure periods are indicated by *horizontal bars*. *Time scale bars* are 200 s

sustained increase in $[Ca^{2+}]_i$ also occurs in the presence of CPA (in Ca^{2+}-free media) suggests that some inhibition of plasma membrane Ca^{2+} extrusion is also likely. Determining which of these pathways are indeed responsible for the sustained Ca^{2+} release from internal stores seen acidic conditions clearly requires further investigation.

Effects of combining acidic stimuli with anoxia and aglycaemia

When acidosis was combined with anoxia, or with both anoxia and aglycaemia, there was a systematic increase in the amplitude of the Ca^{2+} transient (Fig. 13). The effects of acidosis are therefore potentiated by loss of oxygen and loss of glucose both of which are conditions present in ischaemia. There are likely to be a number of factors contributing to this effect. In analysing the cause of the Ca^{2+} transient in anoxia, aglycaemia and acidosis, we found that this transient was exclusively dependent on extracellular Ca^{2+} and was strongly inhibited by BCTC and AMG 9810, but was not inhibited by voltage-gated Ca^{2+}-channel blockers (Ni^{2+}). The major source of Ca^{2+} influx would therefore again seem to be mainly via TRPV1. We did, however, note that amiloride also reduced the Ca^{2+} transient under these conditions. A role for ASICs would therefore seem to be more prominent in response to anoxic–aglycaemic–acidosis than to acidosis alone. One possible explanation for this is that oxygen and glucose deprivation has recently been reported to both increase the amplitude and slow the inactivation of ASIC1a currents in mouse hippocampal neurones [26]. Thus, the amount of Ca^{2+} influx through ASIC1a may be enhanced. Further factors which we anticipate will also contribute to the enhancement of the Ca^{2+} transient by anoxia and aglycaemia include rather more general changes to Ca^{2+} metabolism including inhibition of plasma membrane Ca^{2+} extrusion and inhibition of SR Ca^{2+} uptake [34]. Moderate inhibition of both SERCA and plasma membrane Ca^{2+} ATPase (PMCA) pumps occurs fairly rapidly in anoxia and corresponds to decline in cytosolic ATP levels [34, 35]. These factors probably account for the slower recovery of the Ca^{2+} transient observed in anoxic–aglycaemic–acidosis compared to that seen in acidosis alone. Indeed, we also noted that anoxia both enhanced the $[Ca^{2+}]_i$ response to capsaicin and prolonged $[Ca^{2+}]_i$ recovery following capsaicin removal (Fig. 11c). Given the prominent role for mitochondria in

Ca^{2+} buffering in these cells [2, 63, 79, 83, 103], one might also anticipate that reduced mitochondrial Ca^{2+} uptake should contribute to the enhanced Ca^{2+} transient. In previous studies, however, we have found that although relatively brief anoxia does cause partial mitochondrial depolarisation, this does not appear to affect the capacity of mitochondria to take up Ca^{2+} [34, 35]. In summary, the causes of the enhancement of the acid evoked Ca^{2+} transient in anoxia and aglycaemia are likely to be complex, involving the modulation of both Ca^{2+}-influx and Ca^{2+}-efflux pathways and are in need of further investigation.

Even in the presence of anoxia and aglycaemia, it is notable that the Ca^{2+}-influx phase of the response to acidosis is still relatively short-lived ($t_{1/2}$=43 s; Fig. 11). There are a number of possible explanations for this: Firstly, intrinsic inactivation leads to rapid (seconds) decline in ASIC activity [42, 78], secondly, elevated intracellular calcium leads to inactivation of TRPV1, and finally, declining ATP levels may contribute to loss of TRPV1 activity [91, 94, 112]. What remains after the Ca^{2+} transient has subsided is a sustained elevation of $[Ca^{2+}]_i$ which is largely independent of Ca^{2+} influx. Aglycaemia and anoxia alone can also induce a sustained increase in $[Ca^{2+}]_i$. The response to the combination of all three 'stimuli' is greater than that observed in response to any single stimulus given in isolation (see Fig. 12). Thus, the effects of anoxia, aglycaemia and acidosis on intracellular Ca^{2+} regulation appear to summate. The cause of the rise in $[Ca^{2+}]_i$ in response to anoxia has been described previously and includes inhibition of both SERCA and PMCA as well as enhanced leak of Ca^{2+} from internal (ER) Ca^{2+} stores [34]. The cause of the sustained rise in response to acidosis has not yet been investigated in full, but our preliminary data indicate that it is likely to involve changes to ER calcium handling and hint at a possible role for the recently discovered G protein-coupled proton receptors.

Conclusions

In this study, we have only investigated events likely to occur early in ischaemia; more prolonged ischaemic conditions are predicted to further disturb Ca^{2+} homeostasis as endogenous glycolytic fuel reserves are depleted, ATP levels collapse and Ca^{2+}-extrusion mechanisms fail completely [34, 35]. What is interesting to note, however, is that even before this stage is reached, anoxia and aglycaemia have a marked influence over cellular Ca^{2+} homeostasis enhancing both the calcium influx and the sustained rise in $[Ca^{2+}]_i$ in response to acidosis. Even under anoxic and aglycaemic conditions, however, the acid evoked Ca^{2+} influx, mediated predominantly via TRPV1, remains relatively short-lived.

Important questions that remain to be addressed are how might the Ca^{2+}-signalling events described here be further influenced by other mediators released in ischaemia (e.g. bradykinin and adenosine), could these support, enhance or prolong the Ca^{2+}-influx phase or is Ca^{2+} influx only relevant in the very early stages of ischaemia? If the latter, what are the functional consequences of the sustained (Ca^{2+}-influx independent) rise in $[Ca^{2+}]_i$ in these cells, can it promote continued release of CGRP or is this only linked to the Ca^{2+}-influx phase? Finding answers to these questions is important if we are to gain a better understanding of the role played by acid-sensing cation channels, calcium stores and calcium signalling in general in sensory neurone function under ischaemic conditions.

Acknowledgements This work was supported by a grant from the Wellcome Trust (KJB) and a Deutsche Forschungsgemeinschaft research fellowship (HE3678/1-1 to M. H.).

Open Access This article is distributed under the terms of the Creative Commons Attribution Noncommercial License which permits any noncommercial use, distribution, and reproduction in any medium, provided the original author(s) and source are credited.

References

1. Ahern GP, Brooks IM, Miyares RL, Wang XB (2005) Extracellular cations sensitize and gate capsaicin receptor TRPV1 modulating pain signaling. J Neurosci 25:5109–5116
2. Åkerman KEO, Nicholls DG (1983) Physiological and bioenergetic aspects of mitochondrial Ca transport. Rev Physiol Biochem Pharmacol 95:149–201
3. Altier C, Zamponi GW (2004) Targeting Ca^{2+} channels to treat pain: T-type versus N-type. Trends Pharmacol Sci 25:465–470
4. Altier C, Zamponi GW (2008) Signaling complexes of voltage-gated calcium channels and G protein-coupled receptors. J Recept Signal Transduct Res 28:71–81
5. Baker DG, Coleridge HM, Coleridge JC, Nerdrum T (1980) Search for a cardiac nociceptor: stimulation by bradykinin of sympathetic afferent nerve endings in the heart of the cat. J Physiol 306:519–536
6. Balnave CD, Vaughan-Jones RD (2000) Effect of intracellular pH on spontaneous Ca^{2+} sparks in rat ventricular myocytes. J Physiol 528(Pt 1):25–37
7. Beedle AM, Hamid J, Zamponi GW (2002) Inhibition of transiently expressed low- and high-voltage-activated calcium channels by trivalent metal cations. J Membr Biol 187:225–238
8. Benham CD, Davis JB, Randall AD (2002) Vanilloid and TRP channels: a family of lipid-gated cation channels. Neuropharmacology 42:873–888
9. Benjamin ER, Pruthi F, Olanrewaju S, Shan S, Hanway D, Liu X, Cerne R, Lavery D, Valenzano KJ, Woodward RM, Ilyin VI (2006) Pharmacological characterization of recombinant N-type calcium channel (Cav2.2) mediated calcium mobilization using FLIPR. Biochem Pharmacol 72:770–782
10. Benson CJ, Eckert SP, McCleskey EW (1999) Acid-evoked currents in cardiac sensory neurons: a possible mediator of myocardial ischemic sensation. Circ Res 84:921–928
11. Bevan S, Hothi S, Hughes G, James IF, Rang HP, Shah K, Walpole CS, Yeats JC (1992) Capsazepine: a competitive

antagonist of the sensory neurone excitant capsaicin. Br J Pharmacol 107:544–552
12. Bevan S, Yeats J (1991) Protons activate a cation conductance in a sub-population of rat dorsal root ganglion neurones. J Physiol 433:145–161
13. Bezprozvanny I, Tsien RW (1995) Voltage-dependent blockade of diverse types of voltage-gated Ca2+ channels expressed in Xenopus oocytes by the Ca2+ channel antagonist mibefradil (Ro 40-5967). Mol Pharmacol 48:540–549
14. Biagi BA, Enyeart JJ (1990) Gadolinium blocks low- and high-threshold calcium currents in pituitary cells. Am J Physiol 259: C515–C520
15. Buckler KJ, Vaughan-Jones RD (1994) Effects of hypercapnia on membrane potential and intracellular calcium in rat carotid body type I cells. J Physiol 478(Pt 1):157–171
16. Caterina MJ, Julius D (2001) The vanilloid receptor: a molecular gateway to the pain pathway. Annu Rev Neurosci 24:487–517
17. Caterina MJ, Schumacher MA, Tominaga M, Rosen TA, Levine JD, Julius D (1997) The capsaicin receptor: a heat-activated ion channel in the pain pathway. Nature 389:816–824
18. Chen CC, England S, Akopian AN, Wood JN (1998) A sensory neuron-specific, proton-gated ion channel. Proc Natl Acad Sci USA 95:10240–10245
19. Chu XP, Miesch J, Johnson M, Root L, Zhu XM, Chen D, Simon RP, Xiong ZG (2002) Proton-gated channels in PC12 cells. J Neurophysiol 87:2555–2561
20. Cobbe SM, Poole-Wilson PA (1980) The time of onset and severity of acidosis in myocardial ischaemia. J Mol Cell Cardiol 12:745–760
21. Cobbe SM, Poole-Wilson PA (1980) Tissue acidosis in myocardial hypoxia. J Mol Cell Cardiol 12:761–770
22. Cox DA, Vita JA, Treasure CB, Fish RD, Selwyn AP, Ganz P (1989) Reflex increase in blood pressure during the intracoronary administration of adenosine in man. J Clin Invest 84:592–596
23. Del Bianco E, Santicioli P, Tramontana M, Maggi CA, Cecconi R, Geppetti P (1991) Different pathways by which extracellular Ca2+ promotes calcitonin gene-related peptide release from central terminals of capsaicin-sensitive afferents of guinea pigs: effect of capsaicin, high K+ and low pH media. Brain Res 566:46–53
24. Dibner-Dunlap ME, Kinugawa T, Thames MD (1993) Activation of cardiac sympathetic afferents: effects of exogenous adenosine and adenosine analogues. Am J Physiol 265:H395–H400
25. Franco-Cereceda A, Kallner G, Lundberg JM (1993) Capsazepine-sensitive release of calcitonin gene-related peptide from C-fibre afferents in the guinea-pig heart by low pH and lactic acid. Eur J Pharmacol 238:311–316
26. Gao J, Duan B, Wang DG, Deng XH, Zhang GY, Xu L, Xu TL (2005) Coupling between NMDA receptor and acid-sensing ion channel contributes to ischemic neuronal death. Neuron 48:635–646
27. Gavva NR, Tamir R, Qu Y, Klionsky L, Zhang TJ, Immke D, Wang J, Zhu D, Vanderah TW, Porreca F, Doherty EM, Norman MH, Wild KD, Bannon AW, Louis JC, Treanor JJ (2005) AMG 9810 [(E)-3-(4-t-butylphenyl)-N-(2, 3-dihydrobenzo[b][1, 4] dioxin-6-yl)acrylamide], a novel vanilloid receptor 1 (TRPV1) antagonist with antihyperalgesic properties. J Pharmacol Exp Ther 313:474–484
28. Geppetti P, Tramontana M, Patacchini R, Del Bianco E, Santicioli P, Maggi CA (1990) Neurochemical evidence for the activation of the 'efferent' function of capsaicin-sensitive nerves by lowering of the pH in the guinea-pig urinary bladder. Neurosci Lett 114:101–106
29. Groth M, Helbig T, Grau V, Kummer W, Haberberger RV (2006) Spinal afferent neurons projecting to the rat lung and pleura express acid sensitive channels. Respir Res 7:96
30. Grynkiewicz G, Poenie M, Tsien RY (1985) A new generation of Ca^{2+} indicators with greatly improved fluorescence properties. J Biol Chem 260:3440–3450
31. Gu Q, Lee LY (2006) Characterization of acid signaling in rat vagal pulmonary sensory neurons. Am J Physiol Lung Cell Mol Physiol 291:L58–L65
32. Gunthorpe MJ, Benham CD, Randall A, Davis JB (2002) The diversity in the vanilloid (TRPV) receptor family of ion channels. Trends Pharmacol Sci 23:183–191
33. Helliwell RJ, McLatchie LM, Clarke M, Winter J, Bevan S, McIntyre P (1998) Capsaicin sensitivity is associated with the expression of the vanilloid (capsaicin) receptor (VR1) mRNA in adult rat sensory ganglia. Neurosci Lett 250:177–180
34. Henrich M, Buckler KJ (2008) Effects of anoxia and aglycemia on cytosolic calcium regulation in rat sensory neurons. J Neurophysiol 100:456–473
35. Henrich M, Buckler KJ (2008) Effects of anoxia, aglycemia, and acidosis on cytosolic Mg^{2+}, ATP, and pH in rat sensory neurons. Am J Physiol Cell Physiol 294:C280–C294
36. Hinkle PM, Shanshala ED 2nd, Nelson EJ (1992) Measurement of intracellular cadmium with fluorescent dyes. Further evidence for the role of calcium channels in cadmium uptake. J Biol Chem 267:25553–25559
37. Hua F, Ricketts BA, Reifsteck A, Ardell JL, Williams CA (2004) Myocardial ischemia induces the release of substance P from cardiac afferent neurons in rat thoracic spinal cord. Am J Physiol Heart Circ Physiol 286:H1654–H1664
38. Huang CW, Tzeng JN, Chen YJ, Tsai WF, Chen CC, Sun WH (2007) Nociceptors of dorsal root ganglion express proton-sensing G-protein-coupled receptors. Mol Cell Neurosci 36:195–210
39. Huang WC, Swietach P, Vaughan-Jones RD, Ansorge O, Glitsch MD (2008) Extracellular acidification elicits spatially and temporally distinct Ca2+ signals. Curr Biol 18:781–785
40. Hwang SW, Oh U (2007) Current concepts of nociception: nociceptive molecular sensors in sensory neurons. Curr Opin Anaesthesiol 20:427–434
41. Immke DC, McCleskey EW (2001) Lactate enhances the acid-sensing Na^{+} channel on ischemia-sensing neurons. Nat Neurosci 4:869–870
42. Immke DC, McCleskey EW (2003) Protons open acid-sensing ion channels by catalyzing relief of Ca^{2+} blockade. Neuron 37:75–84
43. Jordt SE, Tominaga M, Julius D (2000) Acid potentiation of the capsaicin receptor determined by a key extracellular site. Proc Natl Acad Sci USA 97:8134–8139
44. Julius D, Basbaum AI (2001) Molecular mechanisms of nociception. Nature 413:203–210
45. Jung J, Hwang SW, Kwak J, Lee SY, Kang CJ, Kim WB, Kim D, Oh U (1999) Capsaicin binds to the intracellular domain of the capsaicin-activated ion channel. J Neurosci 19:529–538
46. Krishtal O (2003) The ASICs: signaling molecules? Modulators? Trends Neurosci 26:477–483
47. Krishtal OA, Pidoplichko VI (1980) A receptor for protons in the nerve cell membrane. Neuroscience 5:2325–2327
48. Krishtal OA, Pidoplichko VI (1981) A receptor for protons in the membrane of sensory neurons may participate in nociception. Neuroscience 6:2599–2601
49. Lansman JB (1990) Blockade of current through single calcium channels by trivalent lanthanide cations. Effect of ionic radius on the rates of ion entry and exit. J Gen Physiol 95:679–696
50. Li YJ, Peng J (2002) The cardioprotection of calcitonin gene-related peptide-mediated preconditioning. Eur J Pharmacol 442:173–177
51. Liu L, Simon SA (1994) A rapid capsaicin-activated current in rat trigeminal ganglion neurons. Proc Natl Acad Sci USA 91:738–741

52. Liu M, Willmott NJ, Michael GJ, Priestley JV (2004) Differential pH and capsaicin responses of Griffonia simplicifolia IB4 (IB4)-positive and IB4-negative small sensory neurons. Neuroscience 127:659–672
53. Lou YP, Lundberg JM (1992) Inhibition of low pH evoked activation of airway sensory nerves by capsazepine, a novel capsaicin-receptor antagonist. Biochem Biophys Res Commun 189:537–544
54. Ludwig MG, Vanek M, Guerini D, Gasser JA, Jones CE, Junker U, Hofstetter H, Wolf RM, Seuwen K (2003) Proton-sensing G-protein-coupled receptors. Nature 425:93–98
55. Lukyanetz EA, Stanika RI, Koval LM, Kostyuk PG (2003) Intracellular mechanisms of hypoxia-induced calcium increase in rat sensory neurons. Arch Biochem Biophys 410:212–221
56. Lundberg JM, Franco-Cereceda A, Alving K, Delay-Goyet P, Lou YP (1992) Release of calcitonin gene-related peptide from sensory neurons. Ann N Y Acad Sci 657:187–193
57. Mamet J, Baron A, Lazdunski M, Voilley N (2002) Proinflammatory mediators, stimulators of sensory neuron excitability via the expression of acid-sensing ion channels. J Neurosci 22:10662–10670
58. Marsh SJ, Stansfeld CE, Brown DA, Davey R, McCarthy D (1987) The mechanism of action of capsaicin on sensory C-type neurons and their axons in vitro. Neuroscience 23:275–289
59. Marzouk SA, Buck RP, Dunlap LA, Johnson TA, Cascio WE (2002) Measurement of extracellular pH, K^+, and lactate in ischemic heart. Anal Biochem 308:52–60
60. Mayer EA, Gebhart GF (1994) Basic and clinical aspects of visceral hyperalgesia. Gastroenterology 107:271–293
61. McIntyre P, McLatchie LM, Chambers A, Phillips E, Clarke M, Savidge J, Toms C, Peacock M, Shah K, Winter J, Weerasakera N, Webb M, Rang HP, Bevan S, James IF (2001) Pharmacological differences between the human and rat vanilloid receptor 1 (VR1). Br J Pharmacol 132:1084–1094
62. Mlinar B, Enyeart JJ (1993) Block of current through T-type calcium channels by trivalent metal cations and nickel in neural rat and human cells. J Physiol 469:639–652
63. Nicholls DG (1978) The regulation of extramitochondrial free calcium ion concentration by rat liver mitochondria. Biochem J 176:463–474
64. Nikonenko I, Bancila M, Bloc A, Muller D, Bijlenga P (2005) Inhibition of T-type calcium channels protects neurons from delayed ischemia-induced damage. Mol Pharmacol 68:84–89
65. Ohta T, Komatsu R, Imagawa T, Otsuguro K, Ito S (2005) Molecular cloning, functional characterization of the porcine transient receptor potential V1 (pTRPV1) and pharmacological comparison with endogenous pTRPV1. Biochem Pharmacol 71:173–187
66. Owsianik G, Talavera K, Voets T, Nilius B (2006) Permeation and selectivity of TRP channels. Annu Rev Physiol 68:685–717
67. Page AJ, Brierley SM, Martin CM, Price MP, Symonds E, Butler R, Wemmie JA, Blackshaw LA (2005) Different contributions of ASIC channels 1a, 2, and 3 in gastrointestinal mechanosensory function. Gut 54:1408–1415
68. Pan HL, Longhurst JC, Eisenach JC, Chen SR (1999) Role of protons in activation of cardiac sympathetic C-fibre afferents during ischaemia in cats. J Physiol 518(Pt 3):857–866
69. Pinchenko VO, Kostyuk PG, Kostyuk EP (2005) Influence of external pH on two types of low-voltage-activated calcium currents in primary sensory neurons of rats. Biochim Biophys Acta 1724:1–7
70. Rotto DM, Stebbins CL, Kaufman MP (1989) Reflex cardiovascular and ventilatory responses to increasing H^+ activity in cat hindlimb muscle. J Appl Physiol 67:256–263
71. Sah DW, Bean BP (1994) Inhibition of P-type and N-type calcium channels by dopamine receptor antagonists. Mol Pharmacol 45: 84–92
72. Sato M, Ikeda K, Yoshizaki K, Koyano H (1991) Response of cytosolic calcium to anoxia and cyanide in cultured glomus cells of newborn rabbit carotid body. Brain Res 551:327–330
73. Schicho R, Donnerer J, Liebmann I, Lippe IT (2005) Nociceptive transmitter release in the dorsal spinal cord by capsaicin-sensitive fibers after noxious gastric stimulation. Brain Res 1039:108–115
74. Spedding M, Kenny B, Chatelain P (1995) New drug binding sites in Ca^{2+} channels. Trends Pharmacol Sci 16:139–142
75. Stapleton SR, Scott RH, Bell BA (1994) Effects of metabolic blockers on Ca^{2+}-dependent currents in cultured sensory neurones from neonatal rats. Br J Pharmacol 111:57–64
76. Steen KH, Steen AE, Reeh PW (1995) A dominant role of acid pH in inflammatory excitation and sensitization of nociceptors in rat skin, in vitro. J Neurosci 15:3982–3989
77. Sugiura T, Dang K, Lamb K, Bielefeldt K, Gebhart GF (2005) Acid-sensing properties in rat gastric sensory neurons from normal and ulcerated stomach. J Neurosci 25:2617–2627
78. Sutherland SP, Benson CJ, Adelman JP, McCleskey EW (2001) Acid-sensing ion channel 3 matches the acid-gated current in cardiac ischemia-sensing neurons. Proc Natl Acad Sci USA 98:711–716
79. Svichar N, Kostyuk P, Verkhratsky A (1997) Mitochondria buffer Ca^{2+} entry but not intracellular Ca^{2+} release in mouse DRG neurones. Neuroreport 8:3929–3932
80. Sylven C (1997) Neurophysiological aspects of angina pectoris. Z Kardiol 86(Suppl 1):95–105
81. Szallasi A (2006) Small molecule vanilloid TRPV1 receptor antagonists approaching drug status: can they live up to the expectations? Naunyn Schmiedebergs Arch Pharmacol 373:273–286
82. Szallasi A, Blumberg PM (1999) Vanilloid (capsaicin) receptors and mechanisms. Pharmacol Rev 51:159–212
83. Thayer SA, Miller RJ (1990) Regulation of the intracellular free calcium concentration in single rat dorsal root ganglion neurones in vitro. J Physiol 425:85–115
84. Thomas RC (2002) The effects of HCl and $CaCl_2$ injections on intracellular calcium and pH in voltage-clamped snail (Helix aspersa) neurons. J Gen Physiol 120:567–579
85. Tjen ALSC, Pan HL, Longhurst JC (1998) Endogenous bradykinin activates ischaemically sensitive cardiac visceral afferents through kinin B_2 receptors in cats. J Physiol 510(Pt 2):633–641
86. Todorovic SM, Lingle CJ (1998) Pharmacological properties of T-type Ca^{2+} current in adult rat sensory neurons: effects of anticonvulsant and anesthetic agents. J Neurophysiol 79:240–252
87. Tombaugh GC, Somjen GG (1996) Effects of extracellular pH on voltage-gated Na^+, K^+ and Ca^{2+} currents in isolated rat CA1 neurons. J Physiol 493(Pt 3):719–732
88. Tominaga M, Caterina MJ, Malmberg AB, Rosen TA, Gilbert H, Skinner K, Raumann BE, Basbaum AI, Julius D (1998) The cloned capsaicin receptor integrates multiple pain-producing stimuli. Neuron 21:531–543
89. Tominaga M, Tominaga T (2005) Structure and function of TRPV1. Pflügers Arch 451:143–150
90. Tomura H, Mogi C, Sato K, Okajima F (2005) Proton-sensing and lysolipid-sensitive G-protein-coupled receptors: a novel type of multi-functional receptors. Cell Signal 17:1466–1476
91. Toth A, Wang Y, Kedei N, Tran R, Pearce LV, Kang SU, Jin MK, Choi HK, Lee J, Blumberg PM (2005) Different vanilloid agonists cause different patterns of calcium response in CHO cells heterologously expressing rat TRPV1. Life Sci 76:2921–2932
92. Tousova K, Vyklicky L, Susankova K, Benedikt J, Vlachova V (2005) Gadolinium activates and sensitizes the vanilloid receptor TRPV1 through the external protonation sites. Mol Cell Neurosci 30:207–217

93. Valenzano KJ, Grant ER, Wu G, Hachicha M, Schmid L, Tafesse L, Sun Q, Rotshteyn Y, Francis J, Limberis J, Malik S, Whittemore ER, Hodges D (2003) N-(4-tertiarybutylphenyl)-4-(3-chloropyridin-2-yl)tetrahydropyrazine-1(2H)-carbox-amide (BCTC), a novel, orally effective vanilloid receptor 1 antagonist with analgesic properties: I. In vitro characterization and pharmacokinetic properties. J Pharmacol Exp Ther 306:377–386
94. Varga A, Bolcskei K, Szoke E, Almasi R, Czeh G, Szolcsanyi J, Petho G (2006) Relative roles of protein kinase A and protein kinase C in modulation of transient receptor potential vanilloid type 1 receptor responsiveness in rat sensory neurons in vitro and peripheral nociceptors in vivo. Neuroscience 140:645–657
95. Viana F, Van den Bosch L, Missiaen L, Vandenberghe W, Droogmans G, Nilius B, Robberecht W (1997) Mibefradil (Ro 40-5967) blocks multiple types of voltage-gated calcium channels in cultured rat spinal motoneurones. Cell Calcium 22:299–311
96. Voets T, Nilius B (2003) The pore of TRP channels: trivial or neglected? Cell Calcium 33:299–302
97. Voets T, Prenen J, Vriens J, Watanabe H, Janssens A, Wissenbach U, Bodding M, Droogmans G, Nilius B (2002) Molecular determinants of permeation through the cation channel TRPV4. J Biol Chem 277:33704–33710
98. Vyklicky L, Knotkova-Urbancova H, Vitaskova Z, Vlachova V, Kress M, Reeh PW (1998) Inflammatory mediators at acidic pH activate capsaicin receptors in cultured sensory neurons from newborn rats. J Neurophysiol 79:670–676
99. Waldmann R, Champigny G, Bassilana F, Heurteaux C, Lazdunski M (1997) A proton-gated cation channel involved in acid-sensing. Nature 386:173–177
100. Waldmann R, Lazdunski M (1998) H^+-gated cation channels: neuronal acid sensors in the NaC/DEG family of ion channels. Curr Opin Neurobiol 8:418–424
101. Wang W, Duan B, Xu H, Xu L, Xu TL (2006) Calcium-permeable acid-sensing ion channel is a molecular target of the neurotoxic metal ion lead. J Biol Chem 281:2497–2505
102. Wang WZ, Chu XP, Li MH, Seeds J, Simon RP, Xiong ZG (2006) Modulation of acid-sensing ion channel currents, acid-induced increase of intracellular Ca^{2+}, and acidosis-mediated neuronal injury by intracellular pH. J Biol Chem 281:29369–29378
103. Werth JL, Thayer SA (1994) Mitochondria buffer physiological calcium loads in cultured rat dorsal root ganglion neurons. J Neurosci 14:348–356
104. Winter J (1998) Brain derived neurotrophic factor, but not nerve growth factor, regulates capsaicin sensitivity of rat vagal ganglion neurones. Neurosci Lett 241:21–24
105. Xiong ZG, Chu XP, Simon RP (2006) Ca^{2+}-permeable acid-sensing ion channels and ischemic brain injury. J Membr Biol 209:59–68
106. Xiong ZG, Pignataro G, Li M, Chang SY, Simon RP (2008) Acid-sensing ion channels (ASICs) as pharmacological targets for neurodegenerative diseases. Curr Opin Pharmacol 8:25–32
107. Xiong ZG, Zhu XM, Chu XP, Minami M, Hey J, Wei WL, MacDonald JF, Wemmie JA, Price MP, Welsh MJ, Simon RP (2004) Neuroprotection in ischemia: blocking calcium-permeable acid-sensing ion channels. Cell 118:687–698
108. Yagi J, Wenk HN, Naves LA, McCleskey EW (2006) Sustained currents through ASIC3 ion channels at the modest pH changes that occur during myocardial ischemia. Circ Res 99:501–509
109. Yan GX, Kleber AG (1992) Changes in extracellular and intracellular pH in ischemic rabbit papillary muscle. Circ Res 71:460–470
110. Yermolaieva O, Leonard AS, Schnizler MK, Abboud FM, Welsh MJ (2004) Extracellular acidosis increases neuronal cell calcium by activating acid-sensing ion channel 1a. Proc Natl Acad Sci USA 101:6752–6757
111. Zahner MR, Li DP, Chen SR, Pan HL (2003) Cardiac vanilloid receptor 1-expressing afferent nerves and their role in the cardiogenic sympathetic reflex in rats. J Physiol 551:515–523
112. Zhang N, Inan S, Cowan A, Sun R, Wang JM, Rogers TJ, Caterina M, Oppenheim JJ (2005) A proinflammatory chemokine, CCL3, sensitizes the heat- and capsaicin-gated ion channel TRPV1. Proc Natl Acad Sci USA 102:4536–4541
113. Zimmermann K, Reeh PW, Averbeck B (2002) ATP can enhance the proton-induced CGRP release through P2Y receptors and secondary PGE_2 release in isolated rat dura mater. Pain 97:259–265